Inhibition of Ubiquitin Ligase F-box and WD repeat domain-containing 7α (Fbw7α) Causes Hepatosteatosis through the Krüppel-like factor 5 (KLF5)/PPARγ2 Pathway, but not SREBP-1c in Mice

[1]Shin Kumadaki, [1]Tadayoshi Karasawa, [1]Takashi Matsuzaka, [2]Masatsugu Ema, [1]Yoshimi Nakagawa, [1]Masanori Nakakuki, [1]Ryo Saito, [1]Naoya Yahagi, [1]Hitoshi Iwasaki, [1]Hirohito Sone, [1]Kazuhiro Takekoshi, [1]Shigeru Yatoh, [1]Kazuto Kobayashi, [1]Akimitsu Takahashi, [1]Hiroaki Suzuki, [2]Satoru Takahashi, [1]Nobuhiro Yamada, and [1*]Hitoshi Shimano

[1]Department of Internal Medicine (Endocrinology and Metabolism)

[2]Department of Anatomy and Embryology

Graduate School of Comprehensive Human Sciences

University of Tsukuba

1-1-1 Tennodai, Tsukuba, Ibaraki 305-8575, Japan

[*]Corresponding author: Hitoshi Shimano, MD, PhD

1-1-1 Tennodai, Tsukuba, Ibaraki 305-8575, Japan

Tel: +81-29-853-3053; Fax: +81-29-853-3174

E-mail: hshimano@md.tsukuba.ac.jp, shimano-tky@umin.ac.jp

Abstract

F-box and WD repeat domain-containing 7α (Fbw7α) is the substrate recognition component of a ubiquitin ligase that controls the degradation of factors involved in cellular growth, including c-Myc, cyclin E, and c-Jun. In addition, Fbw7α degrades the nuclear form of sterol regulatory element binding protein (SREBP)-1a, a global regulator of lipid synthesis, particularly during mitosis in cultured cells. This study investigated the *in vivo* role of Fbw7α in hepatic lipid metabolism. siRNA knockdown of Fbw7α in mice caused marked hepatosteatosis with the accumulation of triglycerides (TGs). However, inhibition of Fbw7α did not change the level of nuclear SREBP-1 protein or the expression of genes involved in fatty acid synthesis and oxidation. *In vivo* experiments on the gain and loss of Fbw7α function indicated that Fbw7α regulated the expression of peroxisome proliferator-activated receptor (PPAR) γ2 and its target genes involved in fatty acid uptake and triglyceride synthesis. These genes included fatty acid transporter CD36, diacylglycerol acyltransferase 1 (DGAT1), and fat-specific protein 27 (Fsp27). The regulation of PPARγ2 by Fbw7α was mediated, at least in part, by the direct degradation of the Krüppel-like factor 5 (KLF5) protein, upstream of PPARγ2 expression. Hepatic Fbw7α contributes to normal fatty acid and triglyceride metabolism, functions which represent novel aspects of this cell growth regulator.

Introduction

F-box and WD repeat domain-containing 7 (Fbw7) is the component of an evolutionary conserved complex of the Skp1-Cul1-F-box protein ubiquitin ligase (SCF) and is involved in substrate recognition of the complex (1,2). Fbw7 targets several proto-oncogenes that function in cell growth and division pathways, including c-Myc, cyclin E, Notch, and c-Jun (3-7). Fbw7, is perturbed in many human malignancies and is an established tumor suppressor (8-11). Mouse Fbw7 exists in three different isoforms: α, β, and γ. The α isoform is expressed ubiquitously, whereas the β and γ isoforms are restrictedly expressed in the brain, heart, testis, and skeletal muscle (12). Intriguing characteristics of Fbw7α have recently been described by Ericsson et al. who demonstrated that this cell growth regulator also regulated the degradation of the nuclear forms of the sterol regulatory element binding protein (SREBP) family (13,14).

SREBPs, belonging to the bHLH-Zip transcription factor family, are established regulators of lipid synthesis. The unique features

of SREBPs are their rER membrane-bound transcription factors. These factors need to undergo proteolytic cleavage for nuclear transport to activate the expression of genes involved in lipid synthesis. This represents the crucial step for sterol and fatty acid synthetic gene regulation (15-17). The SREBP family includes three isoforms: SREBP-1a, -1c, and -2 (18-20). SREBP-2 governs cellular sterol regulation, whereas hepatic SREBP-1c controls fatty acid and triglyceride synthesis depending on the nutritional state of the liver. SREBP-1a is highly expressed in growing cells and contributes to the synthesis of cholesterol, triglyceride (TG), and phospholipid for the supply of membrane lipids during cell growth (21,22). Nuclear SREBP-1a regulates the cell cycle and growth by itself, indicating its strong association with cell growth (23,24).

Without a proteasome inhibitor such as calpain inhibitor I in cell cultures, nuclear SREBPs are rapidly degraded by the ubiquitin–proteasome pathway after cleavage. Recently, Fbw7 was reported to be the key factor for this degradation of SREBPs in cultured cells (14). SREBP-1a is phosphorylated at several sites depending on the cell cycle and then degraded by the ubiquitin–proteasome system. During mitosis, nuclear SREBP-1a is stabilized, and it activates lipid synthesis to supply membrane lipids (25). Thus, Fbw7 controls the degradation of SREBPs in cultured cells in relation to the cell cycle and growth. However, its physiological roles *in vivo* are yet to be determined. In the present study, the effects of Fbw7α modification on SREBPs and lipid metabolism in the liver were investigated.

Experimental procedures

Materials - Antibodies to phosphorylated c-Jun (Ser63) and Lamin A/C were obtained from Cell Signaling Technology (Beverly, MA USA); antibodies to SREBP-1, c-Jun, Krüppel-like factor 5 (KLF5), and α-tubulin were obtained from Santa Cruz Biotechnology (Santa Cruz, CA USA), and that to Fbw7/hCdc4 was purchased from Abcam (Tokyo, Japan).
N-acetyl-Leu-Leu-norleucinal-CHO (ALLN; calpain inhibitor I) and fenofibrate were purchased from Sigma (St. Louis, MO USA), redivue [α-^{32}P]dCTP from GE Healthcare UK Ltd. (Buckinghamshire, England), and [1-^{14}C]palmitate from PerkinElmer Life Sciences (Waltham, MA USA). Restriction enzymes were obtained from Takara Bio Inc. (Shiga, Japan), and plasmid DNAs for transfection were prepared using the Qiagen Plasmid Midi Kit (Qiagen, Hilden, Germany).

Animal experiments - All animal studies were approved by the Animal Care Committee of the University of Tsukuba. Male C57BL/6J mice (9-

and 14-week-old) were purchased from Clea (Tokyo, Japan), and male B6.V-*Lep* ^{ob}/J (ob/ob) mice (7-week-old) were obtained from Charles River (Kanagawa, Japan). SREBP transgenic mice (13-week-old) overexpressing the active form of human SREBP-1c under the control of the rat phosphoenolpyruvate carboxykinase (PEPCK) promoter (SREBP1c-Tg) were generated as described previously (26). In addition, SREBP-1 knockout mice (SREBP1-KO) (6–8-week-old) were generated as described previously (27). KLF5 flox mice, in which the second exon was flanked by two lox sites, were also prepared and established (Ema M, manuscript in preparation). The mice were housed in colony cages, maintained on a 12-h light/12-h dark cycle, given free access to water and standard chow diet (Oriental Yeast, Tokyo, Japan); the mice were adapted to their new environment for at least one week prior to the experiments. After the adenovirus injection, the mice were housed during the periods indicated and then sacrificed in the non-fasted state. Tissues were isolated immediately, weighed, and stored in liquid nitrogen. Plasma metabolic parameters were measured by using commercial kits according to the manufacturer's instructions (all test kits were obtained from Wako Pure Chemical Industries, Osaka, Japan).

Preparation of recombinant adenovirus - We subcloned Fbw7-specific RNAi constructs using the Fbw7 coding sequence 5′-GCTGAAACTGGAGAGTGTA-3′ into a U6 entry vector (Invitrogen, Carlsbad, CA USA). We then generated the recombinant adenoviral plasmid by homologous recombination with a pAd promoterless vector (Invitrogen). Next, we subcloned peroxisome proliferator-activated receptor (PPAR) γ2-specific RNAi constructs using the PPARγ2 coding sequence 5′-GCCTATGAGCACTTCACAA-3′ and generated the recombinant adenoviral plasmid as described above. We subcloned hemagglutinin-tagged mouse Fbw7α cDNA into the pENTR4 vector (Invitrogen) and generated a recombinant adenoviral plasmid by homologous recombination with a pAd/CMV/V5-DEST vector (Invitrogen). We produced recombinant adenoviruses in HEK-293 cells and purified them by CsCl gradient centrifugation, as described previously (28,29). The recombinant adenovirus expressing the Cre recombinase AxCANCre was produced by Dr. Izumu Saito (Institute of Medical Science, University of Tokyo, Japan) and was obtained from Riken DNA Bank (Tsukuba, Japan).

RNA extraction, northern blot analysis, and quantitative real-time PCR - Total RNA was isolated from mouse livers and primary hepatocytes using the Sepazol RNA I Super

reagent (Nacalai Tesque Inc., Kyoto, Japan). Northern blot analysis was performed using the indicated ^{32}P-labeled probe, as described previously (28,30). First-strand cDNA was synthesized using a High Capacity cDNA Reverse Transcription Kit (Applied Biosystems, Foster City, CA USA), and comparative analysis of mRNA levels was performed using fluorescence-based real-time PCR. Real-time PCR analyses were performed using the ABI 7300 PCR system (Applied Biosystems). Quantification of fat-specific protein 27 (Fsp27) was performed using a Taqman gene expression assay (Applied Biosystems), while quantification of other genes was performed using the SYBR-Green Dye (Nippon Gene, Tokyo, Japan). The relative abundance of each transcript was calculated using a standard curve of cycle thresholds for serial dilutions of a cDNA sample and then normalized to cyclophilin levels (31). The expression levels of cyclophilin used as an internal control in each experiment were not affected by procedures such as siRNA transfection. Primer sequences are described in Supplementary Table S1.

Measurement of metabolic parameters - We measured the plasma levels of glucose, insulin, non-esterified fatty acid (NEFA), TG, total cholesterol (TC), aspartate aminotransferase (AST), and alanine aminotransferase (ALT) as well as the levels of TG and TC in the liver, as described previously (32).

Expression plasmids - The expression plasmid for the human nuclear form of SREBP-1c has been described previously (33). Expression plasmids encoding mouse Fbw7α and KLF5 were generated by PCR amplification, followed by the insertion of cDNAs into pcDNA3.1(+) (Promega). The following primers were used: Fbw7α, 5′-primer 5′-CTTAAGCTTGCCACCATGAATCAGGAACTGCTCTCTGT-3′, 3′-primer 5′-CCGGAATTCTCATTTCATGTCCACATCAAAGTCCAG-3′ and KLF5, 5′-primer 5′-CTTAAGCTTGCCACCATGCCCACGCGGGTGC-3′, 3′-primer 5′-CCGGAATTCTCAGTTCTGGTGGCGCT-3′. Restriction sites *Hind*III and *Eco*RI were added to each 5′-primer and 3′-primer, respectively. PCR products were digested with *Hind*III and *Eco*RI, and then inserted into the respective sites of pcDNA3.1(+). Ligation was performed using a Quick Ligation Kit (New England Biolabs Inc., Ipswich, MA USA).

Cell cultures - Cos-7 cells were cultured in DMEM (Sigma) supplemented with 5% FBS and 1% penicillin–streptomycin (Sigma). For the KLF5 degradation assay, Cos-7 cells were seeded 24 h before transfection in 6-cm plates at a density of 3×10^5 cells/plate. Mouse primary hepatocytes were isolated from male C57BL/6J mice, as described previously (28) and seeded in 10-cm

plates for adenovirus infection and measurement of palmitate uptake.

Cellular uptake of [1-^{14}C]palmitate - [1-^{14}C]palmitate uptake by primary hepatocytes was measured as described previously, but with some modifications (34). Briefly, the isolated hepatocytes were infected with adenovirus for 60 h and incubated for 3 h in a culture medium containing 200 μM palmitate, radiolabeled [1-^{14}C]palmitate (0.1 μCi/ml), 2 μM insulin, and 1% BSA (Sigma). After the 3-h incubation, the cells were washed twice with ice-cold PBS and then scraped into it. Cellular lipids were extracted with chloroform/methanol as described by Bligh and Dyer (35), and the residual radioactivity of each sample was then determined.

KLF5 degradation assay - Each indicated expression plasmid (3 μg) was transfected into Cos-7 cells using the FuGENE 6 reagent (Roche Applied Science, Basel, Switzerland), according to the manufacturer's instructions. After 36 h of transfection, the cells were treated with cycloheximide (100 μg/mL) to stop protein synthesis and then incubated with or without ALLN for the indicated times.

Immunoblot analysis - We performed an immunoblot analysis using the antibodies indicated as described previously (29,36,37). The intensity of each detected band was quantified using the image processing software ImageJ (National Institute of Mental Health, Bethesda, MD USA).

Liver histology - Mouse livers were fixed in 10% neutral buffered formalin and embedded in paraffin. The sections were subjected to standard hematoxylin and eosin staining.

Statistical analyses - All data are expressed as mean ± standard error of the mean (SEM). Statistical analyses were performed using unpaired Student's *t*-test, one sample *t*-test, or two-way ANOVA, followed by Tukey's procedure.

Results

To estimate the contribution of Fbw7 to the physiological regulation of hepatic SREBP-1c and hepatic lipogenesis, Fbw7 was knocked down in murine livers by intravenous injection of adenovirus producing Fbw7 siRNA (Fbw7i). We confirmed that only the Fbw7α isoform was expressed in murine livers and cultured hepatoma cells, and Fbw7i fully suppressed Fbw7α expression in cultured hepatoma cells, as estimated by quantitative real-time PCR (data not shown). In livers of mice infected with Fbw7i, the decrease in Fbw7α level was approximately 70% (Figure 1A). This hepatic Fbw7 knockdown caused fatty liver and a slight, but significant, enlargement of the liver (Figures 1B and 1C).

These mice exhibited no significant changes in food intake, white adipose tissue weight, or body weight compared to animals infected with adenovirus producing LacZ siRNA (LacZi) as a control (Figure 1D and data not shown). Of the plasma metabolic parameters, TG, glucose, and insulin levels were reduced significantly by infection with Fbw7i (Table 1). These data indicated that fatty liver was not likely to be associated with overnutrition or obesity. Hepatosteatosis was confirmed by liver histology (Figure 1E) with a marked increase in the liver content of TG (Figure 1F), but not TC (Figure 1G).

Immunoblot analysis of hepatic nuclear extracts demonstrated that the increase in nuclear SREBP-1 protein by Fbw7 knockdown was minimal whereas c-Jun protein, another target of Fbw7, accumulated markedly without a change in its mRNA level (Figures 2A and 2B). This finding confirmed Fbw7 inactivation. The precursor form of SREBP-1c in the whole cell fraction did not change noticeably. Lack of hepatic SREBP-1 activation by Fbw7α suppression was confirmed by the gene expression pattern estimated by real-time PCR (Figure 2C). With the exception of stearoyl-CoA desaturase 1 (SCD1), mRNA levels of SREBP-1c and SREBP-1 target genes involved in fatty acid synthesis such as acetyl-CoA carboxylase, fatty acid synthase (FAS), and long chain fatty acid elongase 6 (Elovl6) were not up-regulated. There were no changes in the expression of carbohydrate response element binding protein, another transcription factor that controls fatty acid synthesis (Figure 2C). The mRNA levels of PPARα, a crucial regulator of hepatic fatty acid oxidation enzymes, and the PPARα target genes acyl-CoA oxidase and medium chain acyl-CoA dehydrogenase did not change (Figure 2D). In contrast, hepatic expression of PPARγ2 increased significantly by Fbw7 knockdown, while expression of PPARγ1 increased minimally. Consistent with these findings, the expression of aP2, another PPARγ2 target gene, was also up-regulated (Figure 2E). We observed marked increases in the mRNA levels of CD36, a transporter involved in the hepatic uptake of plasma fatty acids, mitochondrial glycerol-3-phosphate acyltransferase (GPAT), and diacylglycerol acyltransferase 1 (DGAT1), an enzyme in TG synthesis (Figure 2F). Fsp27/CIDE-C, a lipid droplet binding protein known to promote lipid accumulation in adipocytes, has recently been reported to contribute to hepatosteatosis as a PPARγ target (38-40). Furthermore, the expression of Fsp27 was enhanced by Fbw7 knockdown (Figure 2F). These data indicated that fatty liver induced by Fbw7 knockdown was caused by an elevation in

fatty acid uptake, TG synthesis, and lipid accumulation, rather than by an increase in *de novo* fatty acid synthesis or a decrease in fatty acid degradation. These genes involved in the accumulation of TG are direct targets of PPARγ2. Consistent with the liver cholesterol content remaining unchanged, SREBP-2 target genes involved in cholesterol metabolism such as low density lipoprotein receptor (LDLR) and HMG-CoA reductase (HMGCR) did not change with Fbw7 knockdown (Figure 3A). Apolipoprotein B and microsomal triglyceride transfer protein involved in TG secretion did not decrease (Figure 3B). Expression of gluconeogenic genes such as PEPCK, glucose-6-phosphatase, and glucose transporter 2 did not change, while glucokinase expression decreased significantly by Fbw7 knockdown (Figure 3C). Phosphorylated protein levels of c-Jun increased by Fbw7 knockdown (Figure 2A). Expression of cytokines such as IL-1β and IL-6 did not change (Figure 3D).

The possibility that SREBP-1 did not contribute to fatty liver induced by Fbw7 knockdown was investigated further in SREBP1-KO. Littermates and SREBP1-KO had similar basal mRNA levels of Fbw7α (Figure 4A). After Fbw7 knockdown, the TG content of SREBP1-KO livers increased to levels comparable to littermates (Figure 4B). Inhibition of Fbw7 function by knockdown was confirmed by the increased levels of c-Jun and phosphorylated c-Jun proteins in nuclear extracts (Figure 4C). Lipogenic enzyme genes such as FAS and SCD1 were not affected by Fbw7 knockdown in SREBP1-KO livers (Figure 4D). Fbw7 knockdown did not alter HMGCR expression or liver cholesterol content (Figure 4E and data not shown). Meanwhile, PPARγ2 and CD36 were up-regulated by Fbw7 knockdown irrespective of the presence or absence of SREBP-1 (Figure 4F), indicating SREBP-1c-independent and PPARγ2-mediated TG accumulation.

Besides its stability in the nucleus, nuclear SREBP-1c protein level is regulated mainly by its mRNA level and cleavage activity of the precursor SREBP-1c protein for nuclear transport. To exclude the possibility that the lack of change in the nuclear SREBP-1 protein by Fbw7 knockdown was attributable to changes in mRNA expression and cleavage activity of the precursor protein, we tested the effect of Fbw7 inhibition on the overexpressed nuclear form of the SREBP-1c protein in transgenic livers (Figure 5). Production of nuclear SREBP-1c was stabilized by the transgene under the control of the PEPCK promoter. However, the amount of transgene SREBP-1c protein in liver nuclei was not elevated by Fbw7 knockdown, whereas c-Jun was accumulated (Figures 5A, 5B and 5C).

Expression of SREBP-1c target genes such as FAS and SCD1 was not elevated consistently (Figure 5D). Nevertheless, after Fbw7i treatment, increased TG content was elevated further, and PPARγ2 expression was markedly up-regulated in SREBP-1c transgenic livers to the same extent as in wild-type livers (Figures 5E and 5F). These data suggested that Fbw7 knockdown did not affect the stability of the hepatic nuclear SREBP-1c protein *in vivo*. To directly evaluate the effects of Fbw7 knockdown on the uptake of fatty acids, mouse primary hepatocytes were prepared and infected with Fbw7i (Figure 6). Direct Fbw7 knockdown in primary hepatocytes increased the expression of PPARγ2 and CD36 (Figures 6A, 6B and 6C), leading to an increase in the estimated uptake of fatty acids (Figure 6D).

Conversely, the effects of Fbw7α overexpression were tested (Figure 7). After the adenoviral overexpression of Fbw7α, liver weight was slightly but significantly reduced, while the change in liver TG content was not significant (Figures 7A, 7B, and 7C). Adenoviral overexpression of Fbw7α decreased c-Jun and its phosphorylated protein, but not its mRNA, confirming the enhancement of Fbw7 activity. Meanwhile, Fbw7α overexpression caused parallel decreases in SREBP-1c mRNA as well as precursor and nuclear proteins (Figures 7D, 7E, and 7F). This finding does not support the enhancement of SREBP-1c protein degradation by Fbw7α *in vivo*. In contrast, Fbw7α overexpression suppressed the expression of PPARγ2 and its target genes CD36, DGAT1/2, and Fsp27, but not GPAT as an SREBP-1 target (Figures 7G and 7H). mRNA levels of HMGCR and LDLR genes were not affected (data not shown). Overall, the effects of Fbw7 overexpression were consistently opposed to its inhibition, including the absence of an impact on SREBP-1c.

To confirm that PPARγ2 was responsible for the Fbw7α-mediated regulation of hepatic TG metabolism, PPARγ2 knockdown was superimposed onto Fbw7α knockdown in fatty liver (Figure 8). In double-knockdown animals, the induction of PPARγ2 expression by Fbw7α knockdown (roughly 50% inhibition) was completely suppressed to the baseline level of the LacZi control (Figures 8A and 8B). As a result, the elevation of PPARγ2 target genes such as CD36, DGAT1, and Fsp27 by Fbw7α knockdown was also inhibited completely by PPARγ2 knockdown, and the elevation of hepatic TG content by Fbw7 knockdown decreased considerably (Figures 8C and 8D). These data indicated that PPARγ2 mediated hepatic TG accumulation in the absence of Fbw7α.

PPARγ2 is not regarded as a direct target protein of Fbw7-mediated degradation because its

expression is repressed by Fbw7α at the transcriptional level. Moreover, the protein lacks the Cdc4 phosphodegron (CPD) consensus (2) in its amino acid sequence as an Fbw7 target. CCAAT/enhancer binding protein (C/EBP) β and KLF5 are known as the transcription factors involved in PPARγ2 expression (41,42). KLF5 has been reported as a new target of Fbw7 (43,44), and KLF5, but not C/EBPβ, which has the CPD consensus in its amino acid sequence (Figure 9A). Adenoviral knockdown or overexpression of Fbw7α consistently up-regulated or suppressed KLF5, respectively (Figure 9B), but not C/EBPβ, as estimated by immunoblot analysis of mouse hepatic proteins (data not shown). Fbw7α-mediated degradation of KLF5 was investigated using the cycloheximide chase assay in Cos-7 cells. Fbw7α enhanced the degradation of the KLF5 protein (Figure 9C). This degradation of the KLF5 protein by Fbw7α was inhibited by the proteasome inhibitor ALLN in a way similar to the degradation of the SREBP-1 protein by Fbw7α (Figures 9D and 9E). These data confirmed KLF5 as an Fbw7 target. Finally, the contribution of KLF5 to the Fbw7–PPARγ2 pathway was estimated using primary hepatocytes from KLF5 flox mice (Figure 10). Treatment of KLF5 flox hepatocytes with recombinant adenovirus expressing Cre recombinase (Ad-Cre) led to the essential deletion of KLF5 mRNA (Figure 10A). KLF5-deleted hepatocytes decreased PPARγ2 expression, establishing KLF5 as an upstream transcription factor of PPARγ2. In control hepatocytes infected with Ad-GFP, PPARγ2 expression was increased by Fbw7i, as observed *in vivo* and returned to the basal level with KLF5 deletion (Figures 10B and 10C). These findings demonstrated that KLF5 mediates the Fbw7–PPARγ2 pathway.

To reveal the pathophysiological situation where Fbw7α regulates PPARγ2, we tested the effect of PPARα activation on pathological fatty liver. Obese mice such as db/db or ob/ob mice with leptin deficiency, exhibited severe hepatosteatosis with marked induction of PPARγ2 (42,45). Fibrates that have a PPARα agonist action ameliorate fatty liver associated with a reduction in PPARγ2. The mechanism for this action has yet to be determined (46). In db/db mice, the level of nuclear Fbw7 protein was low, while KLF5 protein level was high compared with the control C57BL/6 mice. This suggests that Fbw7 contributes to PPARγ2 regulation (data not shown). Furthermore, ob/ob mice were treated with fenofibrate, and this system was examined (Figure 11). Interestingly, the PPARα agonist caused strong induction of the nuclear Fbw7 protein, accompanied by a reduction in the KLF5 protein (Figure 11A). This explains the suppression of PPARγ2 and TG content by

PPARα activation (Figures 11B and 11C).

Discussion

Previous *in vitro* studies have suggested that Fbw7 is involved in the degradation of the nuclear SREBP protein (14). The present study was conducted to estimate the role of Fbw7 on the SREBP-1c system for lipogenesis *in vivo*. Unexpectedly, neither knockdown nor overexpression of Fbw7α contributed to SREBP-1c protein levels in livers although our experimental settings on Fbw7 perturbation were strong enough for c-Jun, another target of Fbw7α. No impact of Fbw7α was observed on the nuclear SREBP-1c protein in the liver for a wide range of amounts of nuclear SREBP-1c protein in both wild type and SREBP-1c transgenic mice livers. This finding discounts the possibility of Fbw7α contributing to *in vivo* regulation of liver SREBP-1c. The precise molecular mechanism for this discrepancy between *in vitro* and *in vivo* data is currently unknown. It has been proposed that the regulation of SREBP-1a stability by Fbw7α in cultured cells may be related to the cell cycle and growth (14). In our experimental setting of Cos-7 cells, the impacts of Fbw7α and the proteasome inhibitor ALLN on SREBP-1 proteins were also observed (Figure 9D). However, the cell growth-linked Fbw7α/SREBP system may not work in the liver, considering the long doubling time of hepatocytes.

The present findings demonstrated that Fbw7α regulated TG metabolism in the liver. The gene expression pattern in Fbw7α-knockdown livers indicated that Fbw7 regulated fatty acid uptake and TG synthesis, but not fatty acid synthesis or degradation, thereby highlighting the linkage of PPARγ2 and its target genes CD36, DGAT1, and Fsp27. In addition, the present study emphasized the physiological role of hepatic PPARγ2 in normal nutrition. In contrast to adipose tissue, PPARγ2 expression is low in the livers of mice on a normal diet. The suppression of PPARγ2 by Fbw7α may contribute to this regulation and prevent unnecessary accumulation of hepatosteatosis during a normal energy state.

PPARγ2 is induced and involved in liver TG content in pathological fatty liver such as in ob/ob and diet-induced obesity (DIO) mice (47-50). However, hepatic Fbw7α expression increased slightly under these conditions of overnutrition (data not shown). Fbw7α overexpression had no effect on fatty liver in ob/ob mice. Fbw7α did not appear to have a crucial effect on the regulation of liver TG content in overnutrition, where PPARγ2 induction occurs mainly through the trans-activation of C/EBPα and β (42). In contrast, PPARα ameliorated fatty liver in these mice with a reduction in PPARγ2. Our data indicated that

Fbw7 may mediate this inhibitory action of PPARα on PPARγ2 and hepatosteatosis.

PPARγ2 is related to insulin resistance in ob/ob and DIO mice (48,49). Overexpression of PPARγ2 in livers ameliorated insulin resistance and decreased plasma levels of glucose and insulin in DIO mice, while ablation of PPARγ2 in ob/ob mice resulted in severe insulin resistance and an increase in plasma glucose levels. In the present study, significant decreases in plasma glucose and insulin were observed in Fbw7 knockdown mice, indicating that insulin sensitivity may be enhanced by up-regulation of hepatic PPARγ2 expression (Table 1).

Furthermore, our findings indicated that KLF5 was a direct target of Fbw7 *in vivo* and *in vitro*. Based on the data from KLF5-deleted hepatocytes, KLF5 could at least partially explain PPARγ2 up-regulation by suppression of hepatic Fbw7α. As shown in Figure 10, the induction of PPARγ2 by Fbw7 knockdown was markedly impaired but slightlyremained in KLF5-deleted hepatocytes. This indicates that there could be some KLF5-independent mechanism. Careful interpretation of this molecular process is required as KLF5 may have various biological effects on cell growth (51,52) and secondary metabolic disturbances. Based on previous reports that c-Myc overexpression in transgenic mice contributed to glucose metabolism (53,54), it is possible that c-Myc, potentially induced by Fbw7i, could be involved in steatosis in Fbw7-knockdown livers.

Fbw7 is thought to be a cell growth regulator. The present study demonstrated an association of Fbw7 with hepatic fatty acid uptake and TG synthesis through PPARγ2 and not with lipogenesis through SREBP-1c. Further investigations are necessary to elucidate the precise roles of this versatile factor in light of the association between the nutritional regulation of lipid metabolism and regulation of cell growth.

References

1. Cardozo, T., and Pagano, M. (2004) *Nat. Rev. Mol. Cell. Biol.* **5**, 739-751
2. Nash, P., Tang, X., Orlicky, S., Chen, Q., Gertler, F. B., Mendenhall, M. D., Sicheri, F., Pawson, T., and Tyers, M. (2001) *Nature*. **414**, 514-521
3. Koepp, D. M., Schaefer, L. K., Ye, X., Keyomarsi, K., Chu, C., Harper, J. W., and Elledge, S. J. (2001) *Science*. **294**, 173-177
4. Nateri, A. S., Riera-Sans, L., Da Costa, C., and Behrens, A. (2004) *Science*. **303**, 1374-1378
5. Oberg, C., Li, J., Pauley, A., Wolf, E., Gurney, M., and Lendahl, U. (2001) *J. Biol. Chem.* **276**, 35847-35853
6. Welcker, M., Orian, A., Jin, J., Grim, J. E., Harper, J. W., Eisenman, R. N., and Clurman, B. E. (2004) *Proc. Natl. Acad. Sci. U S A*. **101**, 9085-9090
7. Yada, M., Hatakeyama, S., Kamura, T., Nishiyama, M., Tsunematsu, R., Imaki, H., Ishida, N., Okumura, F., Nakayama, K., and Nakayama, K. I. (2004) *Embo. J.* **23**, 2116-2125
8. Ekholm-Reed, S., Spruck, C. H., Sangfelt, O., van Drogen, F., Mueller-Holzner, E., Widschwendter, M., Zetterberg, A., and Reed, S. I. (2004) *Cancer Res.* **64**, 795-800
9. Rajagopalan, H., Jallepalli, P. V., Rago, C., Velculescu, V. E., Kinzler, K. W., Vogelstein, B., and Lengauer, C. (2004) *Nature* **428**, 77-81
10. Spruck, C. H., Strohmaier, H., Sangfelt, O., Muller, H. M., Hubalek, M., Muller-Holzner, E., Marth, C., Widschwendter, M., and Reed, S. I. (2002) *Cancer Res.* **62**, 4535-4539
11. Strohmaier, H., Spruck, C. H., Kaiser, P., Won, K. A., Sangfelt, O., and Reed, S. I. (2001) *Nature* **413**, 316-322
12. Matsumoto, A., Onoyama, I., and Nakayama, K. I. (2006) *Biochem. Biophys. Res. Commun.* **350**, 114-119
13. Punga, T., Bengoechea-Alonso, M. T., and Ericsson, J. (2006) *J. Biol. Chem.* **281**, 25278-25286
14. Sundqvist, A., Bengoechea-Alonso, M. T., Ye, X., Lukiyanchuk, V., Jin, J., Harper, J. W., and Ericsson, J. (2005) *Cell Metab.* **1**, 379-391
15. Brown, M. S., Ye, J., Rawson, R. B., and Goldstein, J. L. (2000) *Cell* **100**, 391-398
16. Brown, M. S., and Goldstein, J. L. (1999) *Proc. Natl. Acad. Sci. U S A*. **96**, 11041-11048
17. Brown, M. S., and Goldstein, J. L. (1997) *Cell*. **89**, 331-340
18. Hua, X., Yokoyama, C., Wu, J., Briggs, M. R., Brown, M. S., Goldstein, J. L., and Wang, X.

(1993) *Proc. Natl. Acad. Sci. U S A*. **90**, 11603-11607

19. Tontonoz, P., Kim, J. B., Graves, R. A., and Spiegelman, B. M. (1993) *Mol. Cell. Biol.* **13**, 4753-4759
20. Yokoyama, C., Wang, X., Briggs, M. R., Admon, A., Wu, J., Hua, X., Goldstein, J. L., and Brown, M. S. (1993) *Cell*. **75**, 187-197
21. Horton, J. D. (2002) *Biochem. Soc. Trans.* **30**, 1091-1095
22. Shimano, H. (2002) *Vitam. Horm.* **65**, 167-194
23. Inoue, N., Shimano, H., Nakakuki, M., Matsuzaka, T., Nakagawa, Y., Yamamoto, T., Sato, R., Takahashi, A., Sone, H., Yahagi, N., Suzuki, H., Toyoshima, H., and Yamada, N. (2005) *Mol. Cell Biol.* **25**, 8938-8947
24. Nakakuki, M., Shimano, H., Inoue, N., Tamura, M., Matsuzaka, T., Nakagawa, Y., Yahagi, N., Toyoshima, H., Sato, R., and Yamada, N. (2007) *FEBS J.* **274**, 4440-4452
25. Bengoechea-Alonso, M. T., Punga, T., and Ericsson, J. (2005) *Proc. Natl. Acad. Sci. U S A*. **102**, 11681-11686
26. Shimano, H., Horton, J. D., Shimomura, I., Hammer, R. E., Brown, M. S., and Goldstein, J. L. (1997) *J. Clin. Invest.* **99**, 846-854
27. Shimano, H., Shimomura, I., Hammer, R. E., Herz, J., Goldstein, J. L., Brown, M. S., and Horton, J. D. (1997) *J. Clin. Invest.* **100**, 2115-2124
28. Matsuzaka, T., Shimano, H., Yahagi, N., Kato, T., Atsumi, A., Yamamoto, T., Inoue, N., Ishikawa, M., Okada, S., Ishigaki, N., Iwasaki, H., Iwasaki, Y., Karasawa, T., Kumadaki, S., Matsui, T., Sekiya, M., Ohashi, K., Hasty, A. H., Nakagawa, Y., Takahashi, A., Suzuki, H., Yatoh, S., Sone, H., Toyoshima, H., Osuga, J., and Yamada, N. (2007) *Nat. Med*. **13**, 1193-1202
29. Nakagawa, Y., Shimano, H., Yoshikawa, T., Ide, T., Tamura, M., Furusawa, M., Yamamoto, T., Inoue, N., Matsuzaka, T., Takahashi, A., Hasty, A. H., Suzuki, H., Sone, H., Toyoshima, H., Yahagi, N., and Yamada, N. (2006) *Nat. Med.* **12**, 107-113
30. Matsuzaka, T., Shimano, H., Yahagi, N., Yoshikawa, T., Amemiya-Kudo, M., Hasty, A. H., Okazaki, H., Tamura, Y., Iizuka, Y., Ohashi, K., Osuga, J., Takahashi, A., Yato, S., Sone, H., Ishibashi, S., and Yamada, N. (2002) *J. Lipid Res.* **43**, 911-920
31. Kato, T., Shimano, H., Yamamoto, T., Yokoo, T., Endo, Y., Ishikawa, M., Matsuzaka, T., Nakagawa, Y., Kumadaki, S., Yahagi, N., Takahashi, A., Sone, H., Suzuki, H., Toyoshima, H., Hasty, A. H., Takahashi, S., Gomi, H., Izumi, T., and Yamada, N. (2006) *Cell Metab.* **4**, 143-154

32. Yahagi, N., Shimano, H., Hasty, A. H., Matsuzaka, T., Ide, T., Yoshikawa, T., Amemiya-Kudo, M., Tomita, S., Okazaki, H., Tamura, Y., Iizuka, Y., Ohashi, K., Osuga, J., Harada, K., Gotoda, T., Nagai, R., Ishibashi, S., and Yamada, N. (2002) *J. Biol. Chem.* **277**, 19353-19357

33. Kumadaki, S., Matsuzaka, T., Kato, T., Yahagi, N., Yamamoto, T., Okada, S., Kobayashi, K., Takahashi, A., Yatoh, S., Suzuki, H., Yamada, N., and Shimano, H. (2008) *Biochem. Biophys. Res. Commun.* **368**, 261-266

34. Li, L. O., Mashek, D. G., An, J., Doughman, S. D., Newgard, C. B., and Coleman, R. A. (2006) *J. Biol. Chem.* **281**, 37246-37255

35. Bligh, E. G., and Dyer, W. J. (1959) *Can. J. Biochem. Physiol.* **37**, 911-917

36. Ide, T., Shimano, H., Yahagi, N., Matsuzaka, T., Nakakuki, M., Yamamoto, T., Nakagawa, Y., Takahashi, A., Suzuki, H., Sone, H., Toyoshima, H., Fukamizu, A., and Yamada, N. (2004) *Nat. Cell. Biol.* **6**, 351-357

37. Shimano, H., Yahagi, N., Amemiya-Kudo, M., Hasty, A. H., Osuga, J., Tamura, Y., Shionoiri, F., Iizuka, Y., Ohashi, K., Harada, K., Gotoda, T., Ishibashi, S., and Yamada, N. (1999) *J. Biol. Chem.* **274**, 35832-35839

38. Matsusue, K., Kusakabe, T., Noguchi, T., Takiguchi, S., Suzuki, T., Yamano, S., and Gonzalez, F. J. (2008) *Cell Metab.* **7**, 302-311

39. Nishino, N., Tamori, Y., Tateya, S., Kawaguchi, T., Shibakusa, T., Mizunoya, W., Inoue, K., Kitazawa, R., Kitazawa, S., Matsuki, Y., Hiramatsu, R., Masubuchi, S., Omachi, A., Kimura, K., Saito, M., Amo, T., Ohta, S., Yamaguchi, T., Osumi, T., Cheng, J., Fujimoto, T., Nakao, H., Nakao, K., Aiba, A., Okamura, H., Fushiki, T., and Kasuga, M. (2008) *J. Clin. Invest.* **118**, 2808-2821

40. Puri, V., Konda, S., Ranjit, S., Aouadi, M., Chawla, A., Chouinard, M., Chakladar, A., and Czech, M. P. (2007) *J. Biol. Chem.* **282**, 34213-34218

41. Oishi, Y., Manabe, I., Tobe, K., Tsushima, K., Shindo, T., Fujiu, K., Nishimura, G., Maemura, K., Yamauchi, T., Kubota, N., Suzuki, R., Kitamura, T., Akira, S., Kadowaki, T., and Nagai, R. (2005) *Cell Metab.* **1**, 27-39

42. Schroeder-Gloeckler, J. M., Rahman, S. M., Janssen, R. C., Qiao, L., Shao, J., Roper, M., Fischer, S. J., Lowe, E., Orlicky, D. J., McManaman, J. L., Palmer, C., Gitomer, W. L., Huang, W., O'Doherty, R. M., Becker, T. C., Klemm, D. J., Jensen, D. R., Pulawa, L. K., Eckel, R. H., and Friedman, J. E. (2007) *J. Biol. Chem.* **282**, 15717-15729

43. Liu, N., Li, H., Li, S., Shen, M., Xiao, N., Chen, Y., Wang, Y., Wang, W., Wang, R., Wang,

Q., Sun, J., and Wang, P. (2010) *J. Biol. Chem.* **285**, 18858-18867

44. Zhao, D., Zheng, H. Q., Zhou, Z., and Chen, C. (2010) *Cancer Res.* **70**, 4728-4738
45. Rahimian, R., Masih-Khan, E., Lo, M., van Breemen, C., McManus, B. M., and Dube, G. P. (2001) *Mol. Cell Biochem.* **224**, 29-37
46. Carmona, M. C., Louche, K., Nibbelink, M., Prunet, B., Bross, A., Desbazeille, M., Dacquet, C., Renard, P., Casteilla, L., and Penicaud, L. (2005) *Int. J. Obes. (Lond)* **29**, 864-871
47. Matsusue, K., Haluzik, M., Lambert, G., Yim, S. H., Gavrilova, O., Ward, J. M., Brewer, B., Jr., Reitman, M. L., and Gonzalez, F. J. (2003) *J. Clin. Invest.* **111**, 737-747
48. Medina-Gomez, G., Gray, S. L., Yetukuri, L., Shimomura, K., Virtue, S., Campbell, M., Curtis, R. K., Jimenez-Linan, M., Blount, M., Yeo, G. S., Lopez, M., Seppanen-Laakso, T., Ashcroft, F. M., Oresic, M., and Vidal-Puig, A. (2007) *PLoS Genet.* **3**, e64
49. Uno, K., Katagiri, H., Yamada, T., Ishigaki, Y., Ogihara, T., Imai, J., Hasegawa, Y., Gao, J., Kaneko, K., Iwasaki, H., Ishihara, H., Sasano, H., Inukai, K., Mizuguchi, H., Asano, T., Shiota, M., Nakazato, M., and Oka, Y. (2006) *Science*. **312**, 1656-1659
50. Vidal-Puig, A., Jimenez-Linan, M., Lowell, B. B., Hamann, A., Hu, E., Spiegelman, B., Flier, J. S., and Moller, D. E. (1996) *J. Clin. Invest.* **97**, 2553-2561
51. Nandan, M. O., Chanchevalap, S., Dalton, W. B., and Yang, V. W. (2005) *FEBS Lett.* **579**, 4757-4762
52. Nandan, M. O., Yoon, H. S., Zhao, W., Ouko, L. A., Chanchevalap, S., and Yang, V. W. (2004) *Oncogene* **23**, 3404-3413
53. Riu, E., Ferre, T., Hidalgo, A., Mas, A., Franckhauser, S., Otaegui, P., and Bosch, F. (2003) *FASEB J* **17**, 1715-1717
54. Riu, E., Bosch, F., and Valera, A. (1996) *Proc. Natl. Acad. Sci. U S A*. **93**, 2198-2202

Acknowledgments

We are grateful to Prof. Oike for the helpful discussion. We also thank Dr. Tomotaka Yokoo and Motoki Mikami for the beneficial discussion and support. This work was supported by grants-in-aid from the Ministry of Education, Culture, Sports, Science and Technology of Japan.

Abbreviations

Fbw7, F-box and WD repeat domain-containing 7; SCF, Skp1-Cul1-F-box protein ubiquitin ligase; FAS, fatty acid synthase; Elovl6, long chain fatty acid elongase; SCD, stearoyl-CoA desaturase; SREBP, sterol regulatory element binding protein; LDLR, low density lipoprotein receptor; DGAT, diacylglycerol acyltransferase; GPAT, mitochondrial glycerol-3-phosphate acyltransferase; HMGCR, HMG-CoA reductase; PEPCK, phosphoenolpyruvate carboxykinase; KLF5, Krüppel-like factor 5; C/EBP, CCAAT/enhancer binding protein; CPD, Cdc4 phosphodegron; DIO, diet-induced obesity; ob/ob, B6.V-*Lep*^{ob}/J; TG, triglyceride; TC, total cholesterol; NEFA, non-esterified fatty acid; AST, aspartate aminotransferase; ALT, alanine aminotransferase.

Figure Legends

FIGURE 1. ***In vivo*** **effects of Fbw7 knockdown in livers of C57BL/6J mice.** Eight- to nine-week-old male C57BL/6J mice were infected through the tail vein with adenovirus encoding RNAi targeting Fbw7 (Fbw7i) or LacZ (LacZi) sequences (adenoviral dose of 2.5×10^{11} viral particles per mouse). After 4 days of standard chow feeding, the mice were sacrificed in the non-fasted state.

A: Fbw7 mRNA levels in the livers of mice infected with LacZi or Fbw7i, as determined by real-time PCR (graph) or northern blot analysis (insert). The quantities of mRNA were calculated as the ratio of the cyclophilin level in each cDNA sample. Data are shown as the expression ratio relative to the LacZi control group. *B:* Abdominal (top) and hepatic (bottom) views of mice infected with LacZi or Fbw7i. Liver weights (*C*), epididymal white adipose tissue (WAT) weights (*D*), liver histology (hematoxylin and eosin staining, × 200) (*E*), liver triglyceride (TG) contents (*F*), and liver total cholesterol (TC) contents (*G*) of mice infected with LacZi or Fbw7i. n = 9 per group in (*A*), (*C*), (*D*), and (*F*), and n = 4 per group in (*G*). Statistical analysis was performed using unpaired Student's *t*-test; ** $p < 0.01$ (versus LacZi control group).

FIGURE 2. **Effects of Fbw7 knockdown on the protein and mRNA expression in the livers of C57BL/6J mice.** All mice were infected with Fbw7i or LacZi adenovirus. After 4 days of standard chow feeding the mice were sacrificed in the non-fasted state.

A: Immunoblot analysis of the cleaved nuclear forms of SREBP-1 (nSREBP-1), c-Jun, phosphorylated c-Jun (P-c-Jun), and Lamin A/C as an internal control in nuclear extracts and precursor forms of SREBP-1 (pSREBP-1) and α-tubulin as an internal control in whole cell lysates from mouse livers. Each protein sample was obtained from 3–5 mice infected with LacZi or Fbw7i. Protein levels of the Fbw7i group displayed below each blot are shown as the mean ± SEM of the relative quantity ratios to the LacZi control group in 3–5 independent experiments. The protein quantities were determined as described in the experimental procedures and normalized by the respective internal control. *B:* mRNA levels of cJun. *C:* mRNA levels of SREBP-1c, acetyl-CoA carboxylase (ACC), fatty acid synthase (FAS), long chain fatty acid elongase 6 (Elovl6), stearoyl-CoA desaturase (SCD) 1, and carbohydrate responsive element binding protein (ChREBP). *D:* mRNA levels of PPARα and its regulated genes acyl-CoA oxidase (ACO) and medium chain acyl-CoA dehydrogenase (MCAD). mRNA levels of PPARγ1, PPARγ2, aP2 (*E*), and CD36,

mitochondrial glycerol-3-phosphate acyltransferase (GPAT), diacylglycerol acyltransferase 1/2 (DGAT1/2), and fat-specific protein 27 (Fsp27) (*F*). All RNA samples were extracted from the livers of mice infected with LacZi or Fbw7i. The quantities of mRNA were determined by real-time PCR and normalized by the cyclophilin level in each cDNA sample. mRNA levels are shown as the expression ratio relative to the LacZi control group. n = 3–5 per group in (*A*), n = 4–9 per group in (*C*) and (*F*), n = 4 per group in (*B*) and (*D*), and n = 7–9 per group in (*E*). Statistical analysis was performed using one sample *t*-test in (*A*) and unpaired Student's *t*-test in all other panels; ** $p < 0.01$ and * $p < 0.05$ (versus LacZi control group).

FIGURE 3. **Effects of Fbw7 knockdown on gene expression in the livers of C57BL/6J mice.** All mice were infected with Fbw7i or LacZi adenovirus. After 4 days of standard chow feeding the mice were sacrificed in the non-fasted state.
mRNA levels of LDL receptor (LDLR) and HMG-CoA reductase (HMGCR) (*A*), apolipoprotein B (ApoB) and microsomal triglyceride transfer protein (MTTP) (*B*), glucose-6-phosphatase (G6Pase), phosphoenolpyruvate carboxykinase (PEPCK), glucose transporter 2 (GLUT2), and glucokinase (GK) (*C*), and IL-1β and IL-6 (*D*) in the livers of mice infected with LacZi or Fbw7i determined by real-time PCR. The quantities of mRNA were calculated as the ratio of the cyclophilin level in each cDNA sample. mRNA levels are shown as the expression ratio relative to the LacZi control group. n = 4 per group in (*A*) and (*C*), and n = 8 or 9 per group in (*B*) and (*D*). Statistical analysis was performed using unpaired Student's *t*-test; ** $p < 0.01$ and * $p < 0.05$ (versus LacZi control group).

FIGURE 4. **Effects of Fbw7 knockdown on gene expression and TG contents in the livers of SREBP1-KO.** Six- to eight-week-old male SREBP1-KO and littermates were infected through the tail vein with Fbw7i or LacZi adenovirus (adenoviral dose of 2.5×10^{11} viral particles per mouse). After 4 days of standard chow feeding, the mice were sacrificed in the non-fasted state.
A: Fbw7α mRNA levels in the livers of SREBP1-KO and littermates infected with LacZi or Fbw7i determined by real-time PCR. *B:* Liver TG contents of SREBP1-KO and littermates infected with LacZi or Fbw7i. *C:* Immunoblot analysis of cleaved nSREBP-1, c-Jun, P-c-Jun, and Lamin A/C as an internal control in nuclear extracts from the livers of 4 or 5 mice in each group indicated. Quantification results were obtained as described in the experimental procedures and normalized by the internal control. Relative changes compared to controls (littermates infected with LacZi) are displayed below each blot. The mRNA levels of FAS and SCD1 (*D*), HMG-CoA reductase (HMGCR) (*E*), and PPARγ2 and CD36 (*F*) in the livers of SREBP1-KO and littermates infected with

LacZi or Fbw7i. The quantities of mRNA were determined by real-time PCR and normalized by the cyclophilin level in each cDNA sample. mRNA levels were shown as the expression ratio relative to the LacZi control group. n = 4 or 5 per group in all panels. Statistical analysis was performed using unpaired Student's *t*-test; ** $p < 0.01$ (versus respective LacZi control group).

FIGURE 5. **Effects of Fbw7 knockdown on gene expression and TG contents in the livers of SREBP-1c transgenic mice (SREBP1c-Tg).** Thirteen-week-old male SREBP1c-Tg and littermates were infected through the tail vein with Fbw7i or LacZi adenovirus (adenoviral dose of 2.5×10^{11} viral particles per mouse). After 4 days of standard chow feeding, the mice were sacrificed in the non-fasted state.

A: Fbw7a mRNA levels in the livers of SREBP1c-Tg and littermates infected with LacZi or Fbw7i. *B:* Immunoblot analysis of the cleaved nuclear forms of SREBP-1 (nSREBP1), c-Jun, and Lamin A/C as an internal control in nuclear extracts from the livers of 5 mice in each group indicated. Quantification results were obtained as described in the experimental procedures and normalized by the internal control. Relative changes compared to controls (littermates or SREBP1c-Tg infected with LacZi) are displayed below each blot. mRNA expression of exogenous human SREBP-1c (hSREBP-1c) (*C*) and FAS and SCD1 (*D*) in the livers of SREBP1c-Tg and littermates infected with LacZi or Fbw7i. ND, not detected. *E:* Liver TG contents of SREBP1c-Tg and littermates infected with LacZi or Fbw7i. *F:* mRNA levels of PPARγ2 in the livers of SREBP1c-Tg and littermates infected with LacZi or Fbw7i. mRNA quantities were determined by real-time PCR and calculated as the ratio of the cyclophilin level in each cDNA sample. Data are shown as the expression ratio relative to the LacZi control group. n = 5 per group in all panels. Statistical analysis was performed using unpaired Student's *t*-test; ** $p < 0.01$ and * $p < 0.05$ (versus respective LacZi control group).

FIGURE 6. **Influence of Fbw7 knockdown on fatty acid uptake in mouse primary hepatocytes.** Primary hepatocytes were isolated from C57BL/6J mice and infected with Fbw7i or LacZi adenovirus (1000 virus particles/cell) and cultured for 48 h. [1-^{14}C]palmitate uptake of the treated primary hepatocytes was measured, as indicated in the experimental procedures.

mRNA levels of Fbw7α (*A*), PPARγ2 (*B*), and CD36 (*C*) in mouse primary hepatocytes infected with LacZi or Fbw7i. The quantities of mRNA were determined by real-time PCR and normalized by the cyclophilin level in each cDNA sample. mRNA levels are shown as the expression ratio relative to the LacZi control group. *D:* [1-^{14}C]palmitate incorporation into cellular lipid in mouse primary hepatocytes infected with LacZi or Fbw7i. All experiments were performed using five sets of primary

hepatocytes for each group. Statistical analysis was performed using unpaired Student's *t*-test; ** $p < 0.01$ (versus LacZi control group).

FIGURE 7. ***In vivo*** **effects of Fbw7α overexpression in the livers of C57BL/6J mice.** Fourteen-week-old male C57BL/6J mice were infected through the tail vein with adenovirus encoding GFP (Ad-GFP) as the control or mouse Fbw7α (Ad-Fbw7α) (adenoviral dose of 1.5×10^{11} viral particles per mouse). After 6 days of standard chow feeding, the mice were sacrificed in the non-fasted state.

A: mouse Fbw7α mRNA levels in livers of mice infected with Ad-GFP or Ad-Fbw7α determined by real-time PCR (graph) and Fbw7α protein levels, examined by immunoblot analysis (insert). Liver weights (*B*) and liver TG contents (*C*) of the mice infected with Ad-GFP or Ad-Fbw7α. *D:* Immunoblot analysis of cleaved nuclear forms of SREBP-1 (nSREBP-1), c-Jun, P-c-Jun, and Lamin A/C as an internal control in nuclear extracts, and precursor forms of SREBP-1 (pSREBP-1) and α-tubulin as an internal control in whole cell lysates from mouse livers. Each protein sample was obtained from 3–5 mice infected with Ad-GFP or Ad-Fbw7α. Protein levels of the Ad-Fbw7α group displayed below each blot are shown as the mean ± SEM of the relative quantity ratios to the Ad-GFP control group in 3 independent experiments. The protein quantities were determined as described in the experimental procedures and normalized by the respective internal control. The mRNA levels of SREBP-1c, ACC, FAS, Elovl6, and SCD1 (*E*), c-Jun (*F*), PPARγ1 and PPARγ2 (*G*), and CD36, GPAT, DGAT1/2, and Fsp27 (*H*) in the livers of mice infected with Ad-GFP or Ad-Fbw7α. The quantities of mRNA were determined by real-time PCR and normalized by the cyclophilin level in each cDNA sample. The mRNA levels are shown as the expression ratio relative to the Ad-GFP control group. n = 3 per group in (*D*) and n = 5 per group in all other panels. Statistical analysis was performed using one sample *t*-test in (*A*) and unpaired Student's *t*-test in all other panels; ** $p < 0.01$ and * $p < 0.05$ (versus Ad-GFP control group).

FIGURE 8. **Effects of Fbw7 and PPARγ2 double knockdown on gene expression and TG contents in the livers of C57BL/6J mice.** Nine-week-old male C57BL/6J mice were infected through the tail vein with adenovirus encoding RNAi targeting PPARγ2 (PPARγ2i), Fbw7 (Fbw7i), and/or LacZ (LacZi) sequence (adenoviral dose of 2.5×10^{11} viral particles per mouse). After 4 days of standard chow feeding, the mice were sacrificed in the non-fasted state.

The mRNA levels of Fbw7α (*A*), PPARγ1 and PPARγ2 (*B*), and CD36, DGAT1, and Fsp27 (*C*) in livers of mice treated with LacZi alone (LacZi), Fbw7i and LacZi (Fbw7i), or Fbw7i and PPARγ2i

(Fbw7i + PPARγ2i). *D:* The liver TG contents of these three groups are as described above. The quantities of mRNA were determined by real-time PCR and normalized by the cyclophilin level in each cDNA sample. mRNA levels are shown as the expression ratio relative to the LacZi control group. n = 4 or 5 per group in all panels. Statistical analysis was performed using two-way ANOVA followed by Tukey's procedure; ** $p < 0.01$ and * $p < 0.05$ (versus LacZi) and ## $p < 0.01$ (versus Fbw7i).

FIGURE 9. **Fbw7α-mediated degradation of Krüppel-like factor 5 (KLF5).**
A, Amino acid sequence alignment of the Cdc4 phosphodegron (CPD) in cyclin E, c-Myc, c-Jun, and KLF5. *B*, Immunoblot analysis of KLF5 and Lamin A/C as an internal control in nuclear extracts from the livers of 4 or 5 mice infected with LacZi, Fbw7i, Ad-GFP (GFP), or Ad-Fbw7α (Fbw7α). Quantification results were obtained as described in the experimental procedures and normalized by the internal control. The changes relative to the controls (LacZi or GFP) are displayed below each blot. *C:* Cos-7 cells were transfected with KLF5 in the presence or absence of Fbw7α. Thirty-six hours after transfection, the cells were either lysed directly or incubated in the presence of cycloheximide (100 μg/mL) for the time period indicated to determine KLF5 turnover. The levels of KLF5 were determined by immunoblot analysis. *D:* Cos-7 cells were transfected with the SREBP-1c expression plasmid in the presence or absence of Fbw7α. Thirty-six hours after transfection, the cells were treated with vehicle alone (DMSO) or ALLN (50 μg/mL) for 4 h prior to cell lysis. The protein levels of SREBP-1c, Fbw7α, and α-tubulin were determined by immunoblot analysis. *E:* Cos-7 cells were transfected with the KLF5 expression plasmid in the presence or absence of Fbw7α. Thirty-six hours after transfection, the cells were treated with vehicle alone (DMSO) or ALLN (50 μg/mL) for 4 h prior to cell lysis. The protein levels of KLF5, Fbw7α, and α-tubulin were determined by immunoblot analysis.

FIGURE 10. **Contribution of KLF5 to Fbw7-mediated inhibition of PPARγ2.** Primary hepatocytes prepared from KLF5 flox mice were seeded in 6-cm plates and infected with Fbw7i or LacZi (1000 virus particles/cell) and Ad-GFP as the control or Ad-Cre recombinase encoding adenovirus (Ad-Cre) (300 virus particles/cell). Infected hepatocytes were cultured for 48 h, and the mRNA levels in treated hepatocytes determined by real-time PCR.
The mRNA levels of KLF5 (*A*), Fbw7α (*B*), and PPARγ2 (*C*) in mouse primary hepatocytes infected with LacZi or Fbw7i and Ad-GFP or Ad-Cre. The quantities of mRNA were determined by real-time PCR and normalized by the cyclophilin level in each cDNA sample. mRNA levels are shown as the

expression ratio relative to both the LacZi- and Ad-GFP-infected control groups. All experiments were performed using four sets of primary hepatocytes for each group. Statistical analyses were performed using two-way ANOVA followed by Tukey's procedure; * $p < 0.05$ (versus LacZi of each group) and # $p < 0.05$ (versus LacZi or Fbw7i of Ad-GFP group).

FIGURE 11. **Effects of fenofibrate administration on gene expression and TG contents in the livers of ob/ob mice.** Eight-week-old male ob/ob mice were fed a control diet (ob/ob Feno(−)) or 0.1% fenofibrate diet (ob/ob Feno(+)) for 7 days. All mice were sacrificed in the non-fasted state. *A:* Immunoblot analysis of Fbw7α, KLF5, and Lamin A/C as an internal control in nuclear extracts from the livers of 5 mice in each group indicated. Quantification results were obtained as described in the experimental procedures and normalized by the internal control. The changes relative to the controls (ob/ob Feno(−)) are displayed below each blot. *B:* PPARγ2 mRNA levels in livers of ob/ob mice treated with control or 0.1% fenofibrate diet. The quantities of mRNA were determined by real-time PCR and normalized by the cyclophilin level in each cDNA sample. mRNA levels are shown as the expression ratio relative to the ob/ob Feno(−) control group. *C:* Liver TG contents of ob/ob mice treated with control or 0.1% fenofibrate diet. n = 8 or 9 per group in (*B*) and n = 5 per group in (*C*). Statistical analysis was performed using unpaired Student's *t*-test; ** $p < 0.01$ and * $p < 0.05$ (versus ob/ob Feno(−)).

TABLE 1

Plasma metabolic parameters in the Fbw7 knockdown mice.

Data are the mean ± SEM of 4 male C57BL/6J mice in the non-fasted state at day 4 after adenovirus infection.

Parameter	LacZi	Fbw7i
Body weight (g)	25.3 ± 0.47	24.6 ± 0.15
Glucose (mg/dL)	252 ± 8.3	191 ± 14*
Insulin (pg/mL)	0.30 ± 0.083	0.057 ± 0.036*
TG (mg/dL)	151 ± 6.4	92 ± 1.2**
TC (mg/dL)	67.4 ± 6.9	88.2 ± 6.7
NEFA (mEq/L)	1.21 ± 0.04	1.14 ± 0.08
ALT (Karmen unit)	30 ± 1.6	42 ± 1.0**
AST (Karmen unit)	63 ± 4.8	114 ± 5.4**

* $p < 0.05$ and ** $p < 0.01$ (versus each respective LacZi control).

FIGURE 1

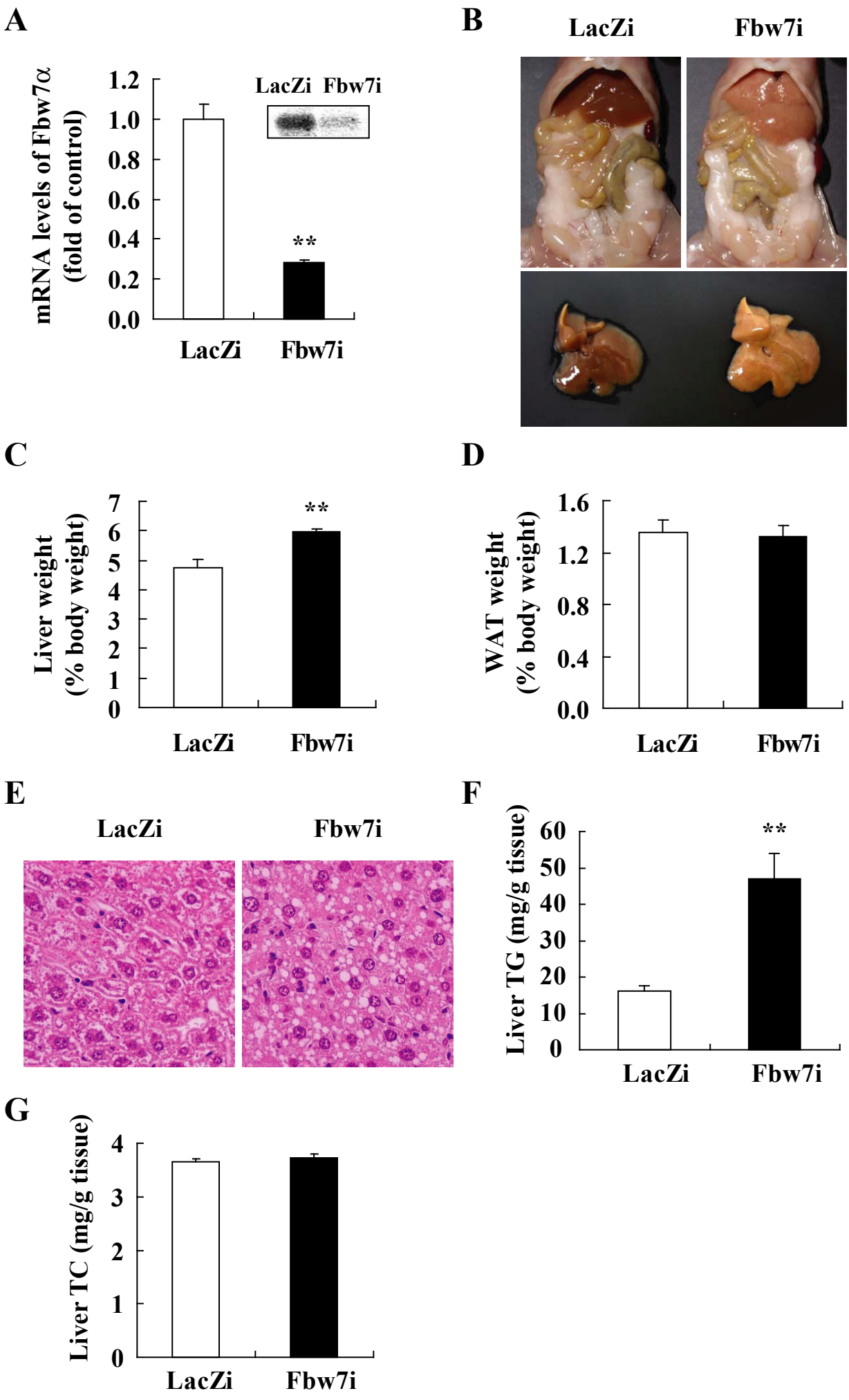
A
mRNA levels of Fbw7α (fold of control)
1.2
1.0
0.8
0.6
0.4
0.2
0.0
LacZi Fbw7i
**
LacZi
Fbw7i
B
LacZi
Fbw7i
C
Liver weight (% body weight)
7
6
5
4
3
2
1
0
**
LacZi
Fbw7i
D
WAT weight (% body weight)
1.6
1.2
0.8
0.4
0.0
LacZi
Fbw7i
E
LacZi
Fbw7i
F
Liver TG (mg/g tissue)
60
50
40
30
20
10
0
**
LacZi
Fbw7i
G
Liver TC (mg/g tissue)
4
3
2
1
0
LacZi
Fbw7i

FIGURE 2

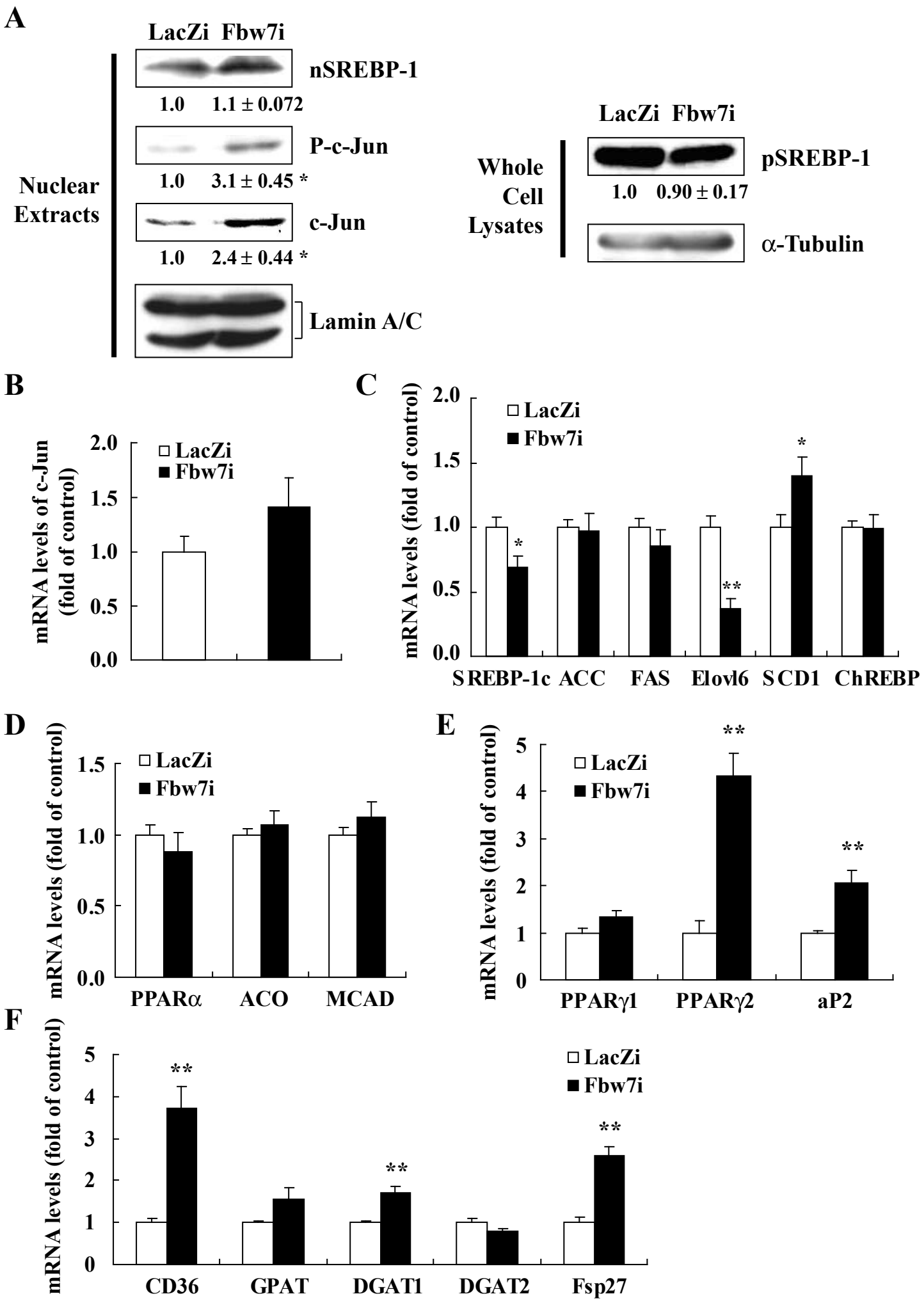
A
LacZi Fbw7i
nSREBP-1
1.0 1.1 ± 0.072
P-c-Jun
1.0 3.1 ± 0.45 *
c-Jun
1.0 2.4 ± 0.44 *
Lamin A/C
Nuclear Extracts
LacZi Fbw7i
pSREBP-1
1.0 0.90 ± 0.17
α-Tubulin
Whole Cell Lysates
B
mRNA levels of c-Jun (fold of control)
LacZi
Fbw7i
C
mRNA levels (fold of control)
SREBP-1c ACC FAS Elovl6 SCD1 ChREBP
D
mRNA levels (fold of control)
PPARα ACO MCAD
E
mRNA levels (fold of control)
PPARγ1 PPARγ2 aP2
F
mRNA levels (fold of control)
CD36 GPAT DGAT1 DGAT2 Fsp27

FIGURE 3

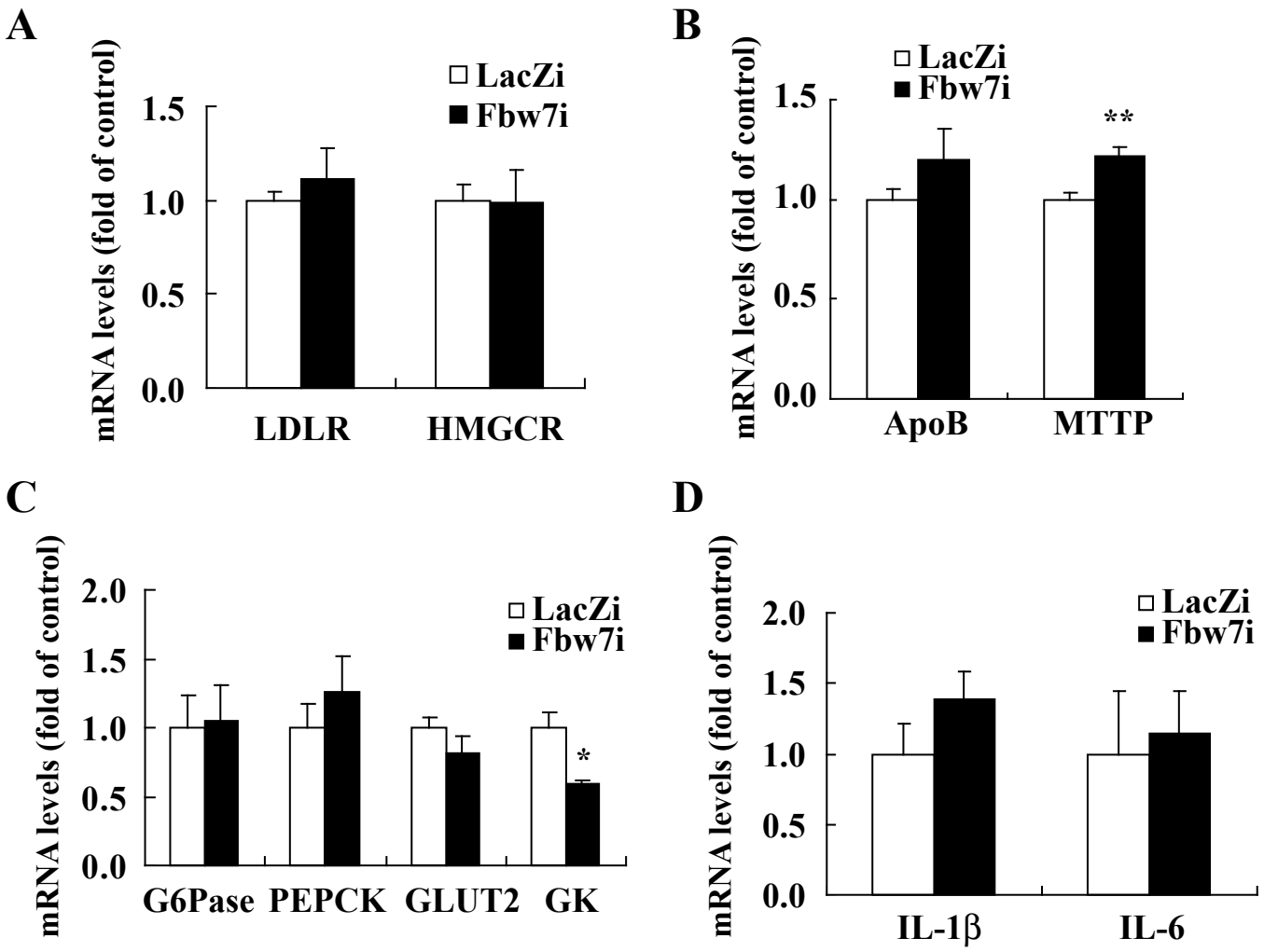
A
mRNA levels (fold of control)
1.5
1.0
0.5
0.0
LacZi
Fbw7i
LDLR
HMGCR
B
mRNA levels (fold of control)
LacZi
Fbw7i
**
ApoB
MTTP
C
mRNA levels (fold of control)
2.0
1.5
1.0
0.5
0.0
LacZi
Fbw7i
*
G6Pase
PEPCK
GLUT2
GK
D
mRNA levels (fold of control)
LacZi
Fbw7i
IL-1β
IL-6

FIGURE 4

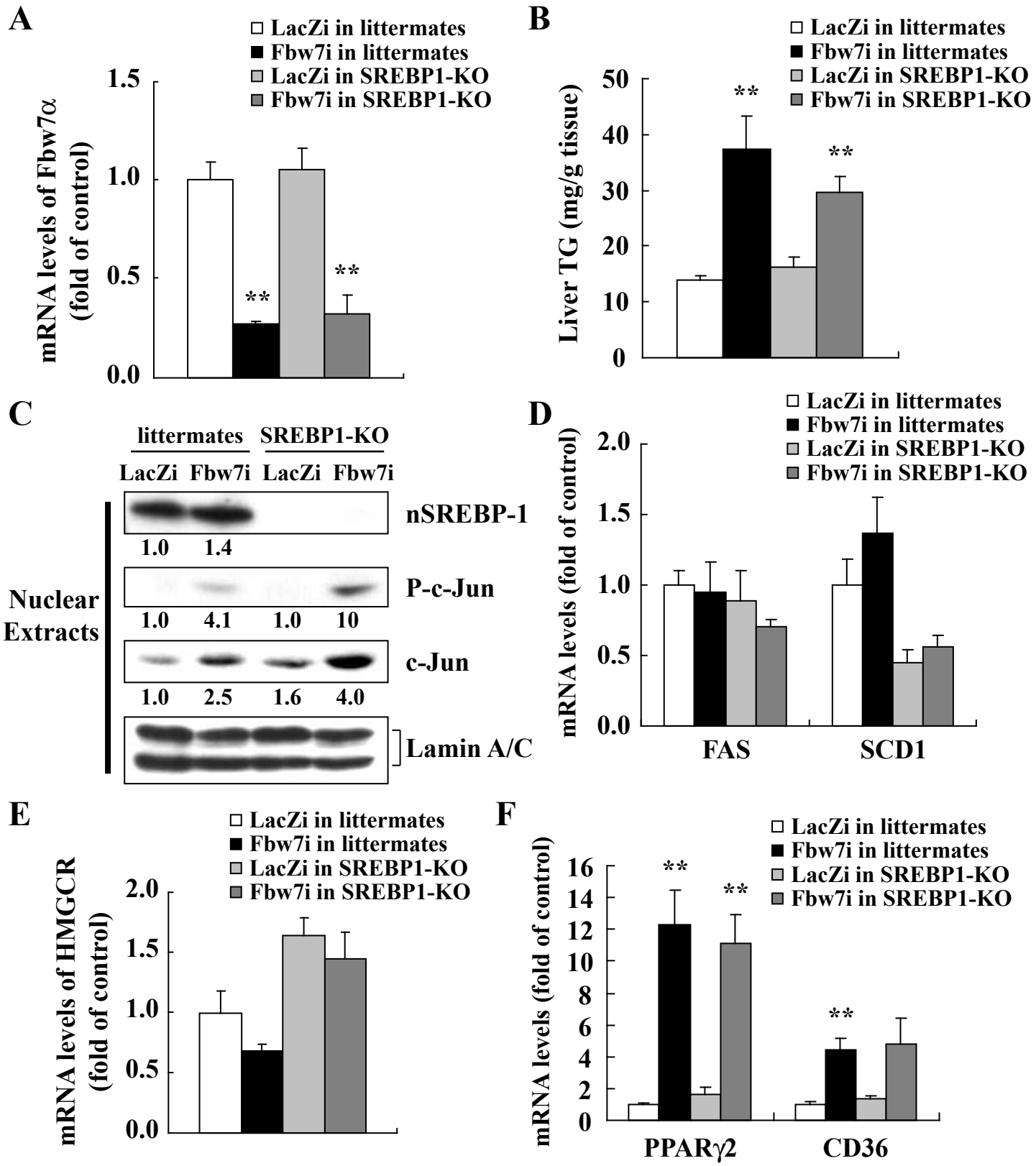
A
LacZi in littermates
Fbw7i in littermates
LacZi in SREBP1-KO
Fbw7i in SREBP1-KO
mRNA levels of Fbw7α (fold of control)
1.5
1.0
0.5
0.0
**
**
B
LacZi in littermates
Fbw7i in littermates
LacZi in SREBP1-KO
Fbw7i in SREBP1-KO
Liver TG (mg/g tissue)
50
40
30
20
10
0
**
**
C
littermates
SREBP1-KO
LacZi Fbw7i LacZi Fbw7i
nSREBP-1
1.0 1.4
P-c-Jun
1.0 4.1 1.0 10
c-Jun
1.0 2.5 1.6 4.0
Lamin A/C
Nuclear Extracts
D
LacZi in littermates
Fbw7i in littermates
LacZi in SREBP1-KO
Fbw7i in SREBP1-KO
mRNA levels (fold of control)
2.0
1.5
1.0
0.5
0.0
FAS
SCD1
E
LacZi in littermates
Fbw7i in littermates
LacZi in SREBP1-KO
Fbw7i in SREBP1-KO
mRNA levels of HMGCR (fold of control)
2.0
1.5
1.0
0.5
0.0
F
LacZi in littermates
Fbw7i in littermates
LacZi in SREBP1-KO
Fbw7i in SREBP1-KO
mRNA levels (fold of control)
16
14
12
10
8
6
4
2
0
**
**
**
PPARγ2
CD36

FIGURE 5

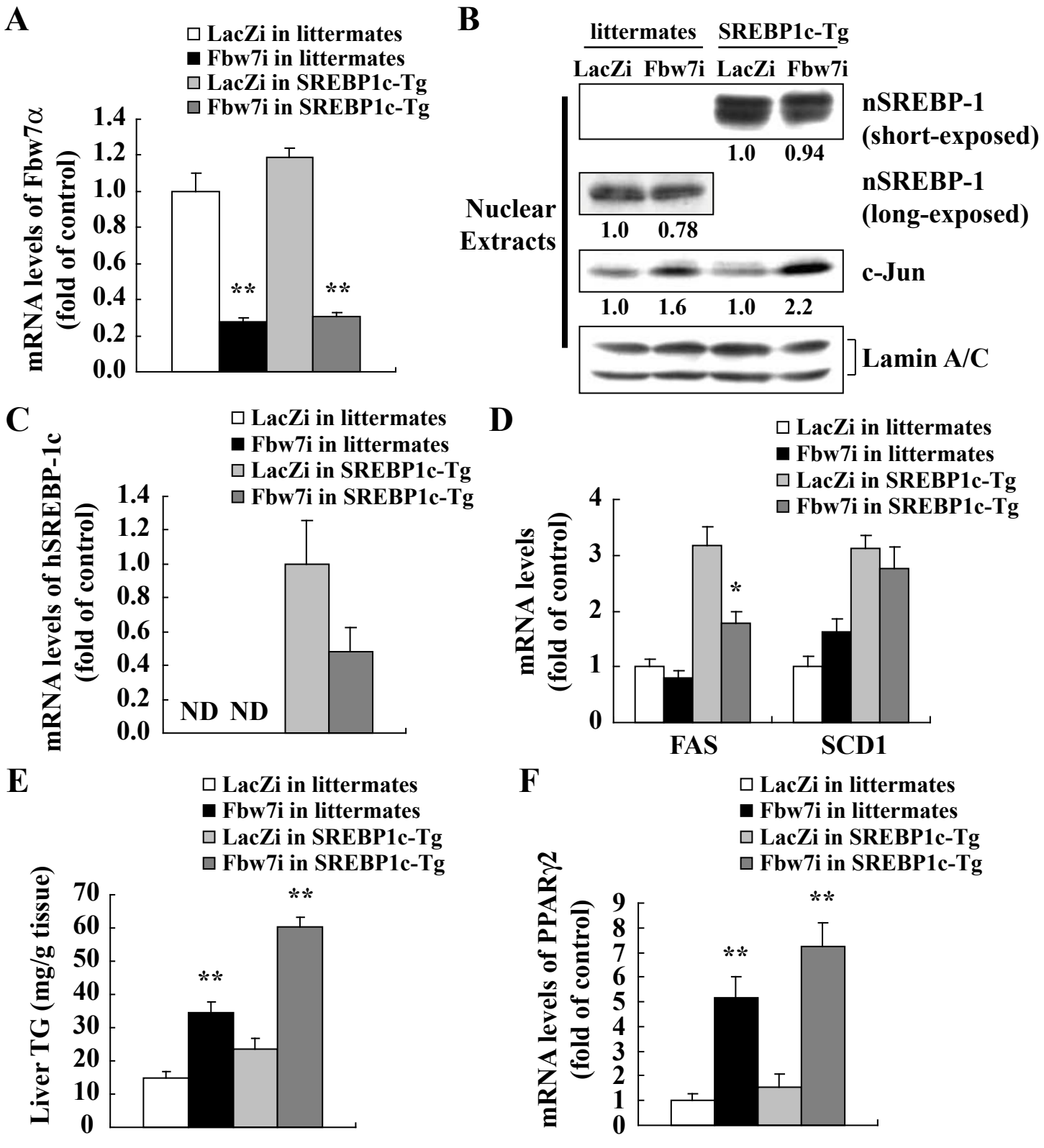
A
LacZi in littermates
Fbw7i in littermates
LacZi in SREBP1c-Tg
Fbw7i in SREBP1c-Tg
mRNA levels of Fbw7α (fold of control)
1.4
1.2
1.0
0.8
0.6
0.4
0.2
0.0
**
**
B
littermates
SREBP1c-Tg
LacZi Fbw7i LacZi Fbw7i
nSREBP-1 (short-exposed)
1.0 0.94
nSREBP-1 (long-exposed)
Nuclear Extracts
1.0 0.78
c-Jun
1.0 1.6 1.0 2.2
Lamin A/C
C
LacZi in littermates
Fbw7i in littermates
LacZi in SREBP1c-Tg
Fbw7i in SREBP1c-Tg
mRNA levels of hSREBP-1c (fold of control)
1.4
1.2
1.0
0.8
0.6
0.4
0.2
0.0
ND ND
D
LacZi in littermates
Fbw7i in littermates
LacZi in SREBP1c-Tg
Fbw7i in SREBP1c-Tg
mRNA levels (fold of control)
4
3
2
1
0
*
FAS
SCD1
E
LacZi in littermates
Fbw7i in littermates
LacZi in SREBP1c-Tg
Fbw7i in SREBP1c-Tg
Liver TG (mg/g tissue)
70
60
50
40
30
20
10
0
**
**
F
LacZi in littermates
Fbw7i in littermates
LacZi in SREBP1c-Tg
Fbw7i in SREBP1c-Tg
mRNA levels of PPARγ2 (fold of control)
9
8
7
6
5
4
3
2
1
0
**
**

FIGURE 6

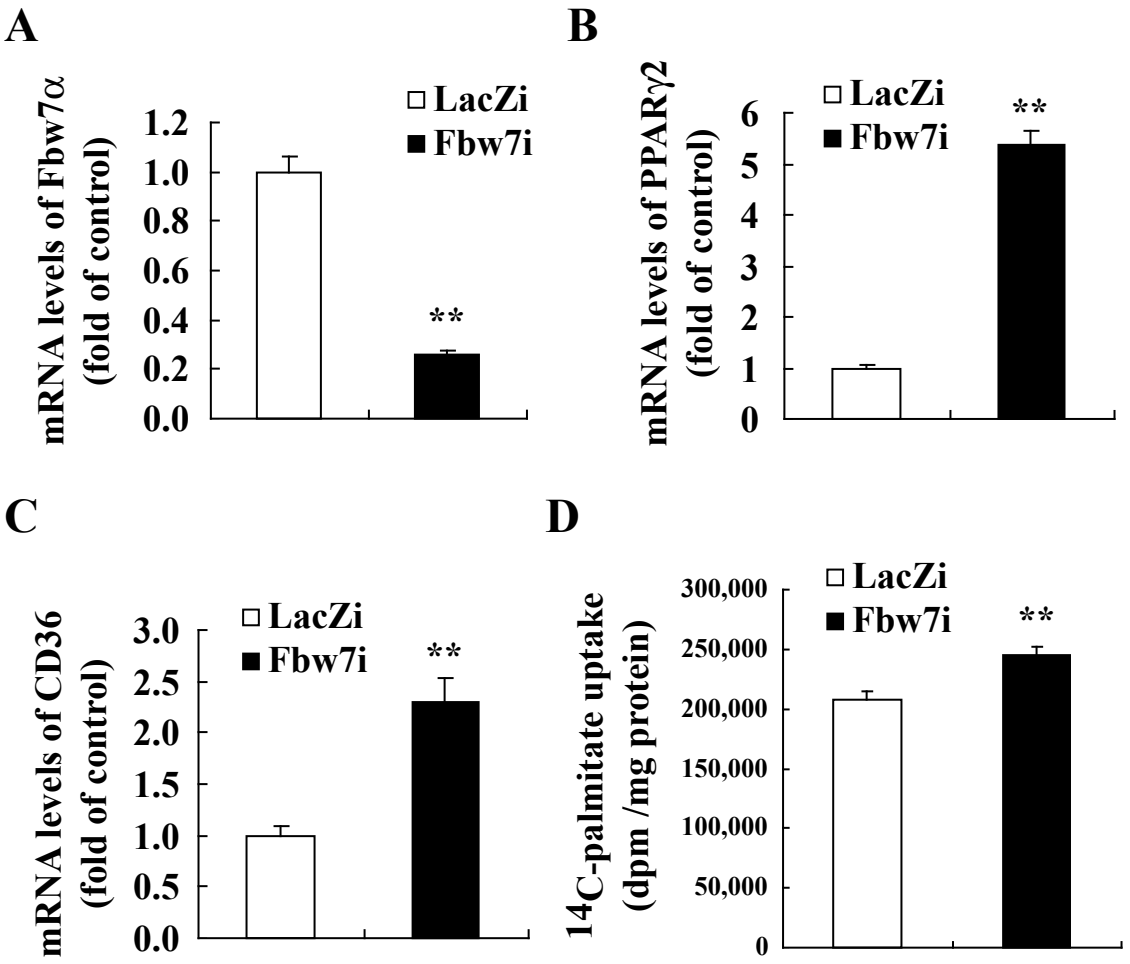
A
mRNA levels of Fbw7α (fold of control)
1.2
1.0
0.8
0.6
0.4
0.2
0.0
LacZi
Fbw7i
**
B
mRNA levels of PPARγ2 (fold of control)
6
5
4
3
2
1
0
LacZi
Fbw7i
**
C
mRNA levels of CD36 (fold of control)
3.0
2.5
2.0
1.5
1.0
0.5
0.0
LacZi
Fbw7i
**
D
14C-palmitate uptake (dpm /mg protein)
300,000
250,000
200,000
150,000
100,000
50,000
0
LacZi
Fbw7i
**

FIGURE 7

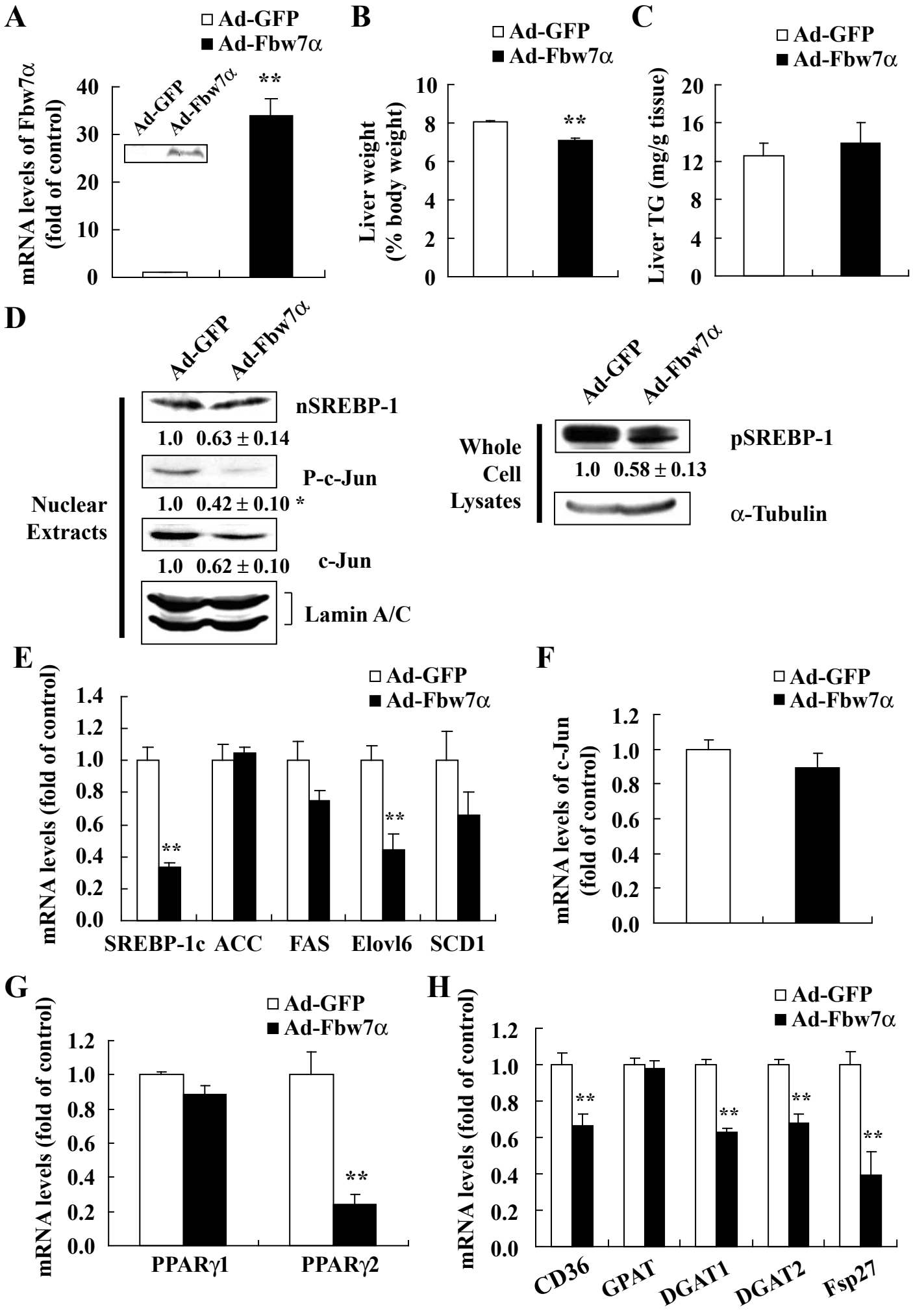
A
Ad-GFP
Ad-Fbw7α
mRNA levels of Fbw7α (fold of control)
Ad-GFP
Ad-Fbw7α
**
B
Ad-GFP
Ad-Fbw7α
Liver weight (% body weight)
**
C
Ad-GFP
Ad-Fbw7α
Liver TG (mg/g tissue)
D
Ad-GFP
Ad-Fbw7α
nSREBP-1
1.0 0.63 ± 0.14
P-c-Jun
1.0 0.42 ± 0.10 *
c-Jun
1.0 0.62 ± 0.10
Lamin A/C
Nuclear Extracts
Ad-GFP
Ad-Fbw7α
pSREBP-1
1.0 0.58 ± 0.13
α-Tubulin
Whole Cell Lysates
E
Ad-GFP
Ad-Fbw7α
mRNA levels (fold of control)
SREBP-1c
ACC
FAS
Elovl6
SCD1
F
Ad-GFP
Ad-Fbw7α
mRNA levels of c-Jun (fold of control)
G
Ad-GFP
Ad-Fbw7α
mRNA levels (fold of control)
PPARγ1
PPARγ2
H
Ad-GFP
Ad-Fbw7α
mRNA levels (fold of control)
CD36
GPAT
DGAT1
DGAT2
Fsp27

FIGURE 8

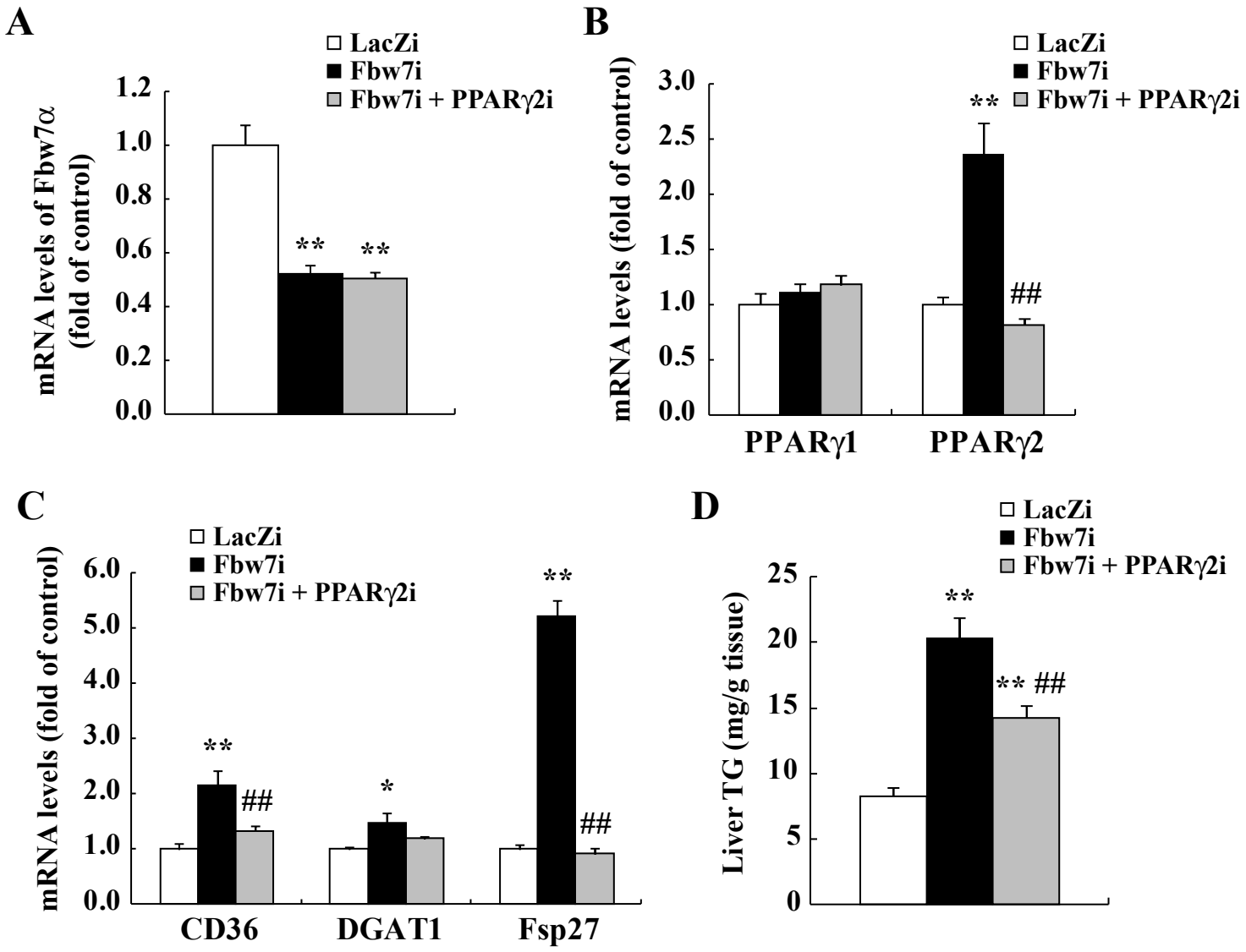
A
LacZi
Fbw7i
Fbw7i + PPARγ2i
mRNA levels of Fbw7α (fold of control)
1.2
1.0
0.8
0.6
0.4
0.2
0.0
**
**
B
LacZi
Fbw7i
Fbw7i + PPARγ2i
mRNA levels (fold of control)
3.0
2.5
2.0
1.5
1.0
0.5
0.0
**
##
PPARγ1
PPARγ2
C
LacZi
Fbw7i
Fbw7i + PPARγ2i
mRNA levels (fold of control)
6.0
5.0
4.0
3.0
2.0
1.0
0.0
**
##
*
**
##
CD36
DGAT1
Fsp27
D
LacZi
Fbw7i
Fbw7i + PPARγ2i
Liver TG (mg/g tissue)
25
20
15
10
5
0
**
** ##

FIGURE 9

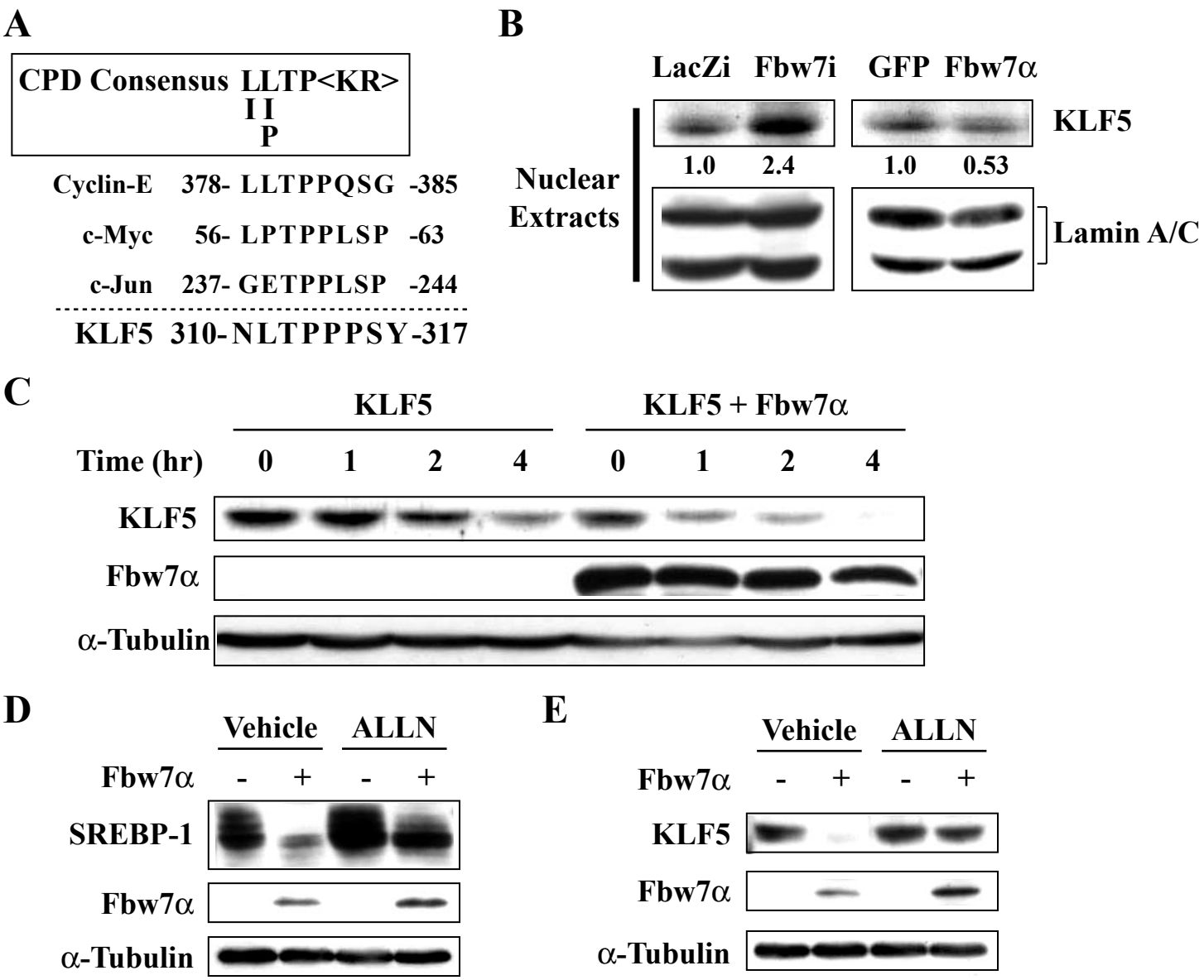
A
CPD Consensus LLTP<KR>
I I
P
Cyclin-E 378- LLTPPQSG -385
c-Myc 56- LPTPPLSP -63
c-Jun 237- GETPPLSP -244
KLF5 310- NLTPPPSY -317
B
LacZi Fbw7i GFP Fbw7α
Nuclear Extracts
KLF5
1.0 2.4 1.0 0.53
Lamin A/C
C
KLF5
KLF5 + Fbw7α
Time (hr) 0 1 2 4 0 1 2 4
KLF5
Fbw7α
α-Tubulin
D
Vehicle ALLN
Fbw7α - + - +
SREBP-1
Fbw7α
α-Tubulin
E
Vehicle ALLN
Fbw7α - + - +
KLF5
Fbw7α
α-Tubulin

FIGURE 10

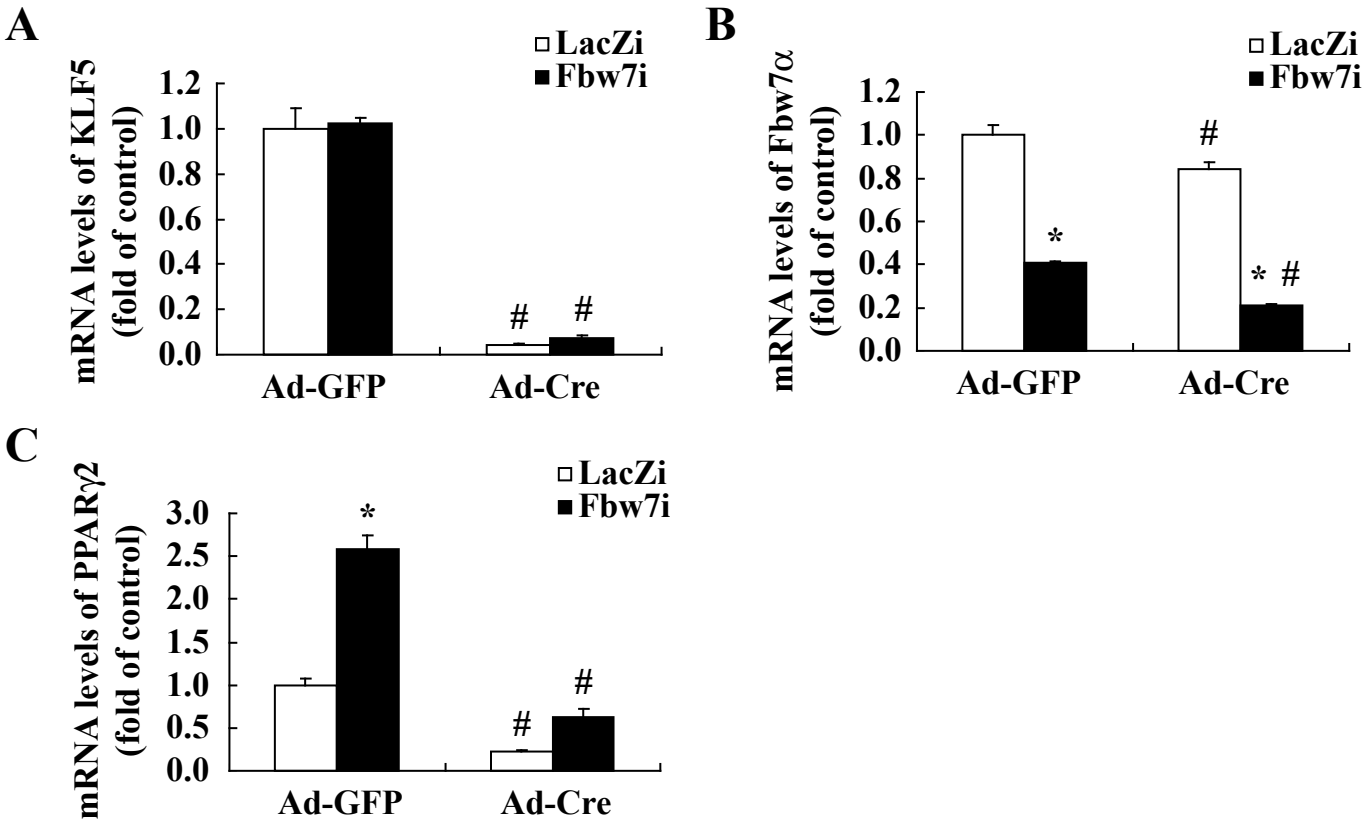
A
mRNA levels of KLF5 (fold of control)
LacZi
Fbw7i
1.2
1.0
0.8
0.6
0.4
0.2
0.0
#
#
Ad-GFP
Ad-Cre
B
mRNA levels of Fbw7α (fold of control)
LacZi
Fbw7i
1.2
1.0
0.8
0.6
0.4
0.2
0.0
#
*
* #
Ad-GFP
Ad-Cre
C
mRNA levels of PPARγ2 (fold of control)
LacZi
Fbw7i
3.0
2.5
2.0
1.5
1.0
0.5
0.0
*
#
#
Ad-GFP
Ad-Cre

FIGURE 11

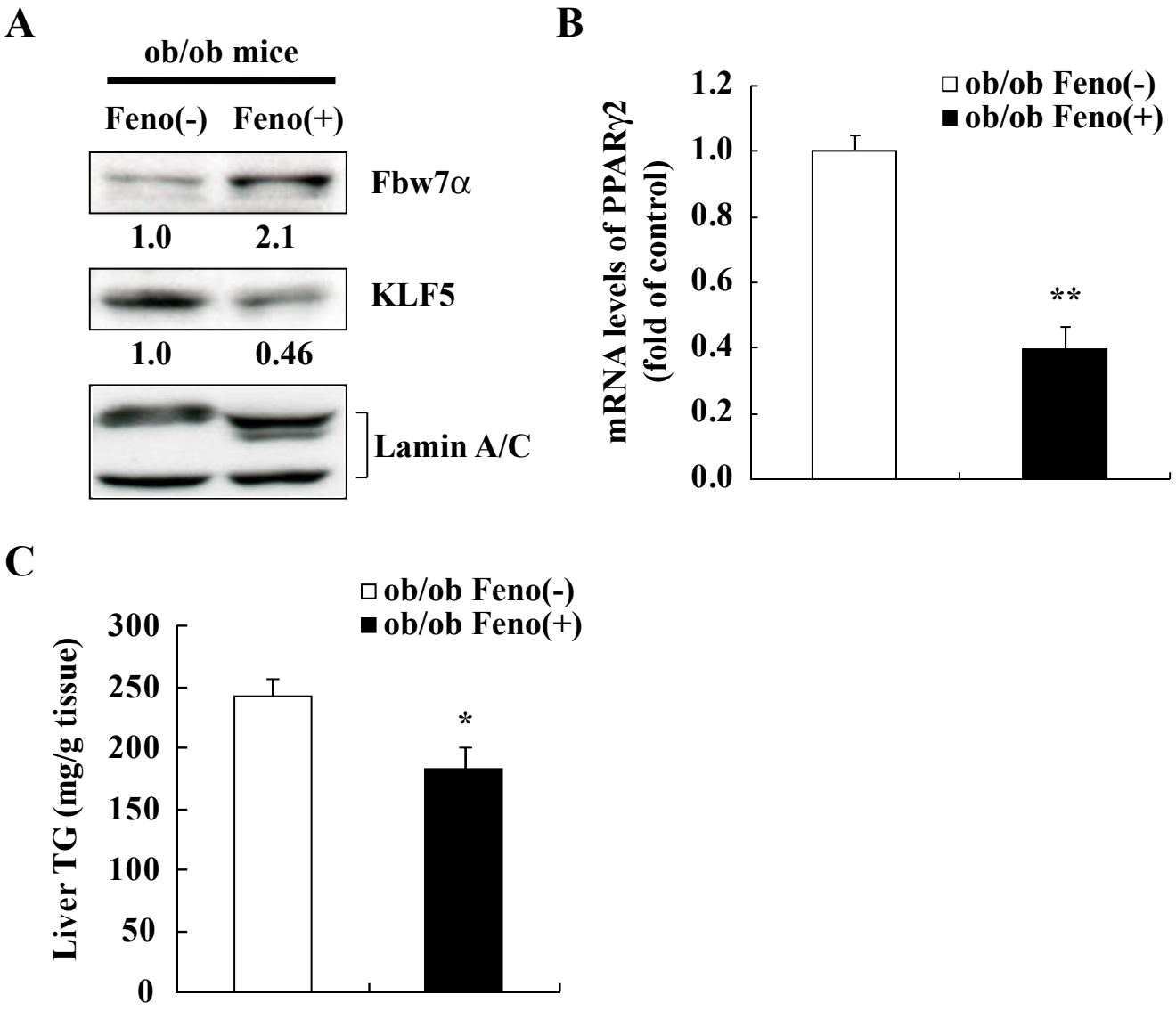
A
ob/ob mice
Feno(-)
Feno(+)
Fbw7α
1.0
2.1
KLF5
1.0
0.46
Lamin A/C
B
ob/ob Feno(-)
ob/ob Feno(+)
mRNA levels of PPARγ2
(fold of control)
1.2
1.0
0.8
0.6
0.4
0.2
0.0
**
C
ob/ob Feno(-)
ob/ob Feno(+)
Liver TG (mg/g tissue)
300
250
200
150
100
50
0
*

Supplementary Table 1. Sequence of primers for quantitative real time-PCR

Gene (mouse)	Sequence of forward primer (5' to 3')	Sequence of reverse primer (5' to 3')
Cyclophilin	TGGCTCACAGTTCTTCATAACCA	ATGACATCCTTCAGTGGCTTGTC
Fbw7α	CTCACCAGCTCTCCTCTCCATT	GCTGAACATGGTACAAGGCCA
SREBP1c	CGGCGCGGAAGCTGT	TGCAATCCATGGCTCCGT
ACC	GGGCACAGACCGTGGTAGTT	CAGGATCAGCTGGGATACTGAGT
FAS	ATCCTGGAACGAGAACACGATCT	AGAGACGTGTCACTCCTGGACTT
Elovl6	CCCGAACTAGGTGACACGAT	CCAGCGACCATGTCTTTGTA
SCD1	AGATCTCCAGTTCTTACACGACCAC	CTTTCATTTCAGGACGGATGTCT
ChREBP	CTGGGGACCTAAACAGGAGC	GAAGCCACCCTATAGCTCCC
LDLR	TGGAGGATGAGAACCGGCT	GCACTGAAAATGGCTTCGTTTA
HMGCR	GACAAGAAGCCTGCTGCCATA	CGTCAACCATAGCTTCCGTAGTT
PPARα	CCTCAGGGTACCACTACGGAGT	GCCGAATAGTTCGCCGAA
ACO	CGATCCAGACTTCCAACATGAG	CCATGGTGGCACTCTTCTTAACA
MCAD	TGCTTTTGATAGAACCAGACCTACAGT	CTTGGTGCTCCACTAGCAGCTT
PPARγ1	GCGGCTGAGAAATCACGTTC	GAATATCAGTGGTTCACCGCTTC
PPARγ2	AACTCTGGGAGATTCTCCTGTTGA	GAAGTGCTCATAGGCAGTGCAT
CD36	CCAAATGAAGATGAGCATAGGACAT	GTTGACCTGCAGTCGTTTTGC
GPAT	GGCTACGTCCGAGTGGATTTT	AACATCATTCGGTCTTGAAGGAA
DGAT1	CGTGGTATCCTGAATTGGT	GGCGCTTCTCAATCTGAAAT
DGAT2	ATCTTCTCTGTCACCTGGCT	ACCTTTCTTGGGCGTGTTCC
KLF5	ACCTTACAGCATCAACATGAACG	TGGCTGAAAATGGTAACAGGTT
G6Pase	GGGCGCAGCAGGTGTATACTAT	CAGAATCCCAACCACAAGATGA
PEPCK	TGTCATCCGCAAGCTGAAGA	TTCGATCCTGGCCACATCTC
GLUT2	GGAACCTTGGCTTTCACTGTCTT	GGAACACCCAAAACATGTCGAT
GK	TCCCTGTAAGGCACGAAGACAT	ATTGCCACCACATCCATCTCA
c-Jun	CCTTCTACGACGATGCCCTC	GGTTCAAGGTCATGCTCTGTTT
aP2	TTTCCTTCAAACTGGGCGTG	AGGGTTATGATGCTCTTCACCTTC
IL-6	TAGTCCTTCCTACCCCAATTTCC	TTGGTCCTTAGCCACTCCTTC
IL-1β	GCAACTGTTCCTGAACTCAACT	ATCTTTTGGGGTCCGTCAACT
ApoB	TTGGCAAACTGCATAGCATCC	TCAAATTGGGACTCTCCTTTAGC
MTTP	AGCTTTGTCACCGCTGTGC	TCCTGCTATGGTTTGTTGGAAGT